

Wilson's disease model establishment  
from human induced pluripotent stem cells

(ヒト誘導多能性幹細胞から作られたウイ  
ルソン病の病態モデル)

2 0 2 1

筑波大学大学院博士課程人間総合科学研究科

宋 丹

筑波大学

博士（医学）学位論文

# Contents

<b>1. Abstract</b> .....	<b>1</b>
<b>2. Introduction</b> .....	<b>3</b>
<b>3. Material and Methods</b> .....	<b>8</b>
<b>3.1. Material</b> .....	<b>8</b>
<b>3.1.1. The information of WD-patient-derived iPSC lines generated in this study (Table 1).</b> .....	<b>8</b>
<b>3.1.2. Primers used for ATP7B transcript 1 amplification and sequence (Table 2)</b> .....	<b>9</b>
<b>3.1.3. Primers used to verify ATP7B mutations in genomic DNA (Table 3).</b> <b>9</b>	<b>9</b>
<b>3.1.4. Taqman probes used in this study (Table 4).</b> .....	<b>10</b>
<b>3.1.5. Primary antibodies used in this study (Table 5)</b> .....	<b>11</b>
<b>3.1.6. Secondary antibodies used in this study (Table 6)</b> .....	<b>12</b>
<b>3.1.7. Chemicals used in this study (Table 7)</b> .....	<b>13</b>
<b>3.1.8. Reagents used in this study (Table 8)</b> .....	<b>14</b>
<b>3.2. Methods</b> .....	<b>17</b>
<b>3.2.1. iPSCs generation and culture</b> .....	<b>17</b>
<b>3.2.2. Microarray assay</b> .....	<b>18</b>
<b>3.2.3. Pluripotency characterization with teratoma formation</b> .....	<b>19</b>
<b>3.2.4. Pluripotency identification with embryonic body formation</b> .....	<b>20</b>
<b>3.2.5. Mutation identification in WD-Hep</b> .....	<b>20</b>
<b>3.2.6. TA-cloning</b> .....	<b>22</b>
<b>3.2.7. Quantitative RT-PCR</b> .....	<b>22</b>
<b>3.2.8. Immunostaining</b> .....	<b>23</b>

3.2.9. Hepatocyte differentiation.....	24
3.2.10. Cell lysate and culture supernatant preparation for Simple Wes	25
3.2.11. Automatic capillary western blot.....	26
3.2.12. Cp secretion-based drug screening.....	27
3.2.13. Oleic acid exposure and retinoids, RXR/RARs agonists treatment.....	28
3.2.14. RNA-Seq .....	28
<b>4. Results .....</b>	<b>30</b>
4.1. Generation and characterization of four WD patient-derived iPSCs..	30
4.2. ATP7B mutation identification in four WD iPSCs .....	35
4.3. Hepatic differentiation of WTC11 iPSC line.....	38
4.4. Hepatic differentiation and characterization of WD iPSCs .....	41
4.5. ATP7B expression in four WD iPSC lines derived hepatocytes.....	44
4.6. Cp expression was consistently decreased in WD iPSCs derived hepatocyte .....	49
4.7. ATP7B expression and Cp secretion in <i>ATP7B</i> deficient iPSC derived hepatocyte.....	54
4.8. ATP7B expression and Cp secretion in R778L homozygous and R778L heterozygous iPSC derived hepatocyte .....	59
4.9. Cp secretion-based drug screening to explore new therapeutic target of WD.....	64
4.10. Transcriptome comparison between WD-Hep and WT-Hep .....	71
4.11. ATRA suppresses oleic acid-induced reactive oxygen species (ROS) production in WD-specific hepatocytes .....	73
<b>5. Discussion .....</b>	<b>83</b>
<b>6. Reference paper .....</b>	<b>88</b>
<b>7. Acknowledgements .....</b>	<b>95</b>

## 1. Abstract

Induced pluripotent stem cells (iPSCs) is a promising tool to study pathophysiological processes *in vitro*. My study was aiming to establish Wilson disease (WD) model with patients derived iPSC line. WD is a copper metabolic disorder, which is caused by defective ATP7B function. Copper chelators are used as the conventional therapies, which usually cause severe side effects and present significant variation in efficacy according to the cohort studies. Thus, exploring new therapeutic medicine for preventing aggravation to liver failure is urgent. Here, I used four iPSC lines generated from WD patients which are carrying compound heterozygous mutations on *ATP7B*. To establish the Wilson's disease hepatic model, WD iPSCs were induced into hepatocyte with a robust differentiation protocol. WD disease features were further identified in WD-specific hepatocyte. Results showed that although the expression level of ATP7B protein was variable among different WD iPSC line derived hepatocytes, the expression and secretion of ceruloplasmin (Cp), which is a downstream copper carrier in plasma, were consistently decreased in WD-specific and ATP7B-deficient hepatocytes. ATP7B loss- and gain-of-functions were further manifested with ATP7B-deficient iPSCs and heterozygous-corrected R778L WD patient-derived iPSCs using CRISPR-Cas9-based gene editing. Cp secretion-based drug screening identified retinoids as promising candidates for rescuing Cp secretion. Furthermore, transcriptome analysis was performed to compare the global gene expression between the healthy donor iPSC derived hepatocytes

and WD-specific hepatocytes. The transcriptome data was showing that the dysregulated genes in the WD-Hep was related to abnormalities of retinoid signaling pathway and lipid metabolism in WD-specific hepatocytes. To further evaluate the therapeutic value of all-trans retinoic acid (ATRA) on fatty liver related disease, I established the steatosis model with WD-specific hepatocyte. Results showed that ATRA could also alleviate reactive oxygen species (ROS) production induced by lipid accumulation in WD-specific hepatocytes treated with oleic acid. These patient-derived iPSC-based hepatic models provide effective platforms to develop potential therapeutics for hepatic steatosis in WD and other fatty liver diseases.

## 2. Introduction

Wilson's disease (WD) (OMIM #277900), an autosomal recessive disorder, is majorly characterized by copper accumulation in liver, leading to a series of metabolic disorders in liver and nervous systems [1]. WD is caused by defective *ATP7B*, which is located on chromosome 13, containing 21 exons, coding a protein of 1,465 amino acids known as copper-transporting P-type ATPase. More than 600 disease-causing mutations have been reported on *ATP7B* gene, which span almost all exons [2, 3], and also presents the pattern of specific mutations dominant in specific ethnic groups [4]. The estimated incidence of WD is about 1:30000 [1, 4], while the carrier frequency is up to 1 in 90. While the etiology for most of the mutations is still unclear.

WD patients are facing lifelong medical treatment. Copper chelators such as Penicillamine, trientine, zinc salt, tetrathiomolybdate, are used as conventional therapies[5-8]. The mechanism for these traditional copper chelators is distinct [9]. For instance, D-penicillamine and Trientine could promote the excretion of copper from the bile duct, while the effect of Zinc is to interfere with the copper up taken from the food[10]. According to the cohort studies, these traditional drugs could cause undesirable side effects, such as bone marrow depression and skin abnormalities [6]. Thus, exploring new therapeutic medicine to prevent aggravation of liver failure is urgent [11, 12].

To study the physiology and pathology of WD, immortalized cell lines [13, 14] and rodent WD models [15-18] were used conventionally; however, there is still a big gap between different species, as well as the different genetic backgrounds among individuals. *Atp7b*<sup>-/-</sup> mouse were conventionally used for WD study [19]. *Atp7b* (-/-) mice showed hepatic metabolic alteration, such as reduced body weight, adiposity, and hepatic steatosis compared with WT controls [20]. According to the clinical reports, about 50% of Wilson's disease patients showed steatosis alteration[9]. This discrepancy indicated that the animal model could not fully recapitulate the disease feature of patients, which promoted us to establish the WD model with human cells. By overexpressing defective ATP7B protein, immortal cell lines have been used to study the individual mutations of ATP7B[14]. While there is a considerable difference in the cellular metabolic state between the immortal cell lines and the actual target cells, it mainly was caused by the different genetic backgrounds.

Induced pluripotent stem cells (iPSCs) is a promising material used for regeneration and pharmacological purpose. With the available differentiation protocol, iPSCs can differentiate into any cell type we need. The consistent differentiation protocol and culture condition could minimize the difference between the bunches. iPSC-derived target cells could provide us with unlimited cell sources, which is invaluable for medicine development.

Patients derived cells have been used for genetic disease studies for decades. Generated from patient somatic cells, patients iPSCs are carrying the same mutations as patient somatic cells. Once differentiated into the target cells types, these cells are supposed to exhibit the corresponding disease phenotypes under the patient genetic background. Great effort has been put into iPSC line establishment from WD patients [21-23]. Patient-derived iPSCs enable us to generate human hepatocytes to study WD physiology and pathology [21-28]. Previous studies mainly focused on high frequent hot spot mutations[29]. With more and more Wilson's disease-related mutations identified, the traditional hotspots study could not meet the clinical needs gradually. Establishing an effective disease modeling protocol is needed to clarify the correlation between mutations and disease phenotype. However, However, due to the limited number of patients used in these studies, which fell short of statistical tests, generally targetable features of WD caused by variable mutations have not been fully identified. It impeded the application of WD iPSC for clinical purposes.

To find a disease feature faithfully recapitulated by the iPSC derived hepatocyte *in vitro* is the key for the disease modeling with patients' iPSC line. In the case of Wilson's disease, the dysfunction of ATP7B presented defective copper transportation capability, which would result in the copper accumulation in the liver or other organs. The regulatory function of ATP7B on copper homeostasis in the liver is by the following two pathways. One way is by forming the copper vesicles eliminated via bile; the other way is by assisting copper incorporated into

Ceruloplasmin (Cp) in the trans-Golgi network secreted into the blood[30]. Cp is a copper-containing plasma ferroxidase synthesized in hepatocytes. Low concentration of serum Cp is generally used as a diagnostic criterion of WD [31, 32]. Cp is a secreted protein of which direct regulatory function on the liver is not well defined. While studies also showed the correlation between the Cp and oxidative stress status. Cp could reduce oxidative stress by preventing reactive oxygen species production[31, 33]. Conversely, Cp expression was also tightly regulated the ROS homeostasis by the posttranscriptional way [33].

In my present study, four patients WD iPSC lines which were carrying compound mutations on ATP7B gene were investigated. Also, one ATP7B-deficient iPSC line generated from a healthy-donor iPSC line by gene editing and a heterozygously mutation-corrected iPSCs from R778L homozygous mutant iPSC line which generated previously were included[24-27]. With these WD-specific and ATP7B-deficient iPSC lines, I was aiming to explore the disease phenotype-genotype correlation and to seek novel therapeutic candidates. WD hepatic models could successfully recapitulate the reduction of Cp expression and secretion. From a small-scale drug screening for rescuing Cp secretion levels in WD-iPSC-derived hepatocytes, I found all-trans retinoic acid (ATRA) and clinically-approved retinoids, as promising candidates. Transcriptome analysis identified differentially-regulated genes in WD-specific hepatocytes that led to abnormalities of retinoid signaling pathways and lipid metabolism. Also, ATRA alleviated reactive oxygen species (ROS) production induced by lipid

accumulation in oleic-acid-treated WD-specific hepatocytes. Based on the central role of Cp in copper and iron homeostasis and its anti-oxidative properties, our results implied that retinoids could prevent or delay the progression of WD related symptoms via regulating Cp expression level.

### 3. Material and Methods

#### 3.1. Material

3.1.1. The information of WD-patient-derived iPSC lines generated in this study (Table 1).

iPSC cell line name	Gender	Age of sampling	Ethnicity	Disease	Origin	Exogenous genes
HPS2807	Female	40s	Japanese	Wilson's disease	Peripheral blood mononuclear cell	Oct3/4, Sox2, Klf4, L-Myc, Lin28, mp53DD, EBNA1
HPS0045	Female	Non-disclosure	Japanese	Wilson's disease	Skin fibroblast	pMXs-Oct3/4, -Sox2, -Klf4, -c-Myc
HPS0049	Male	Non-disclosure	Japanese	Wilson's disease	Skin fibroblast	pMXs-Oct3/4, -Sox2, -Klf4, -c-Myc
HPS0053	Female	Non-disclosure	Japanese	Wilson's disease	Skin fibroblast	pMXs-Oct3/4, -Sox2, -Klf4, -c-Myc

**3.1.2. Primers used for ATP7B transcript 1 amplification and sequence (Table 2).**

	<b>Forward/Reverse primer (5'-3')</b>
Primer 1	F: Tcctctcccgggactttaac/R: cagtggagggtgaccacat
Primer 2	F: Agagcaaagtggctccctta/R: accaacacggagagaaacacc
Primer 3	F: aagtccccacaatcaaccag/R: ggcaatgaacacaaagagca
Primer 4	F: Ctctggcatcctgggtggt/R: ggtgccagtctgtcaaaca
Primer 5	F: aacccaacaagcacatctc/R: atggcgactttctcccttt
Primer 6	F: Aatcgagacgctgtcaag/R: tcagcttggtgagtggag
Primer 7	F: gggacaagtggctctgctc/R: ccgagtacggactctcaggt
Primer 8	F: Tgcttctggctcacacat/R: tcacagctgacagacactgct
Primer 9	F: aggggcttcgtttcagct/R: aacaacattccccaagcaag
Primer 10	F: Tgattgacagaacccttgg/R: ttttagaggaatgacaggaacttt

**3.1.3. Primers used to verify ATP7B mutations in genomic DNA (Table 3).**

<b>Mutation site</b>	<b>Forward/Reverse primer (5'-3')</b>
406	F: gaagggagtgaggacagatca/R: catgcaaggaaagttgcag
456	F: gatggctgagggacaaggta/R: gggcgttcatctctaccag
778	F: gagacacaggtcagccaaca/R: cctgaaggccaggttcttt
832	F: tcagcagctgcacgataaat/R: ttacagtgtccgggttc
952	F: tgtgaagagttctgggaaatca/R: cctgcagaaggagagtgactg
1035	F: tgcaggtgtcttgttctctg/R: ggcctctaagtggtttcc
1262	F: caggagccagggataaactg/R: ctgatggagaggagcacaca

#### 3.1.4. Taqman probes used in this study (Table 4).

<b>Gene name</b>	<b>Assay ID</b>
AFP	Hs01040598_m1
ALB	Hs00609411_m1
SOX17	Hs00751752_s1
ATP7B	Hs01075310_m1
CP	Hs00236810_m1

SERPINA1	Hs00165475_m1
HNF4A	Hs00230853_m1
DLK1	Hs00171584_m1

### 3.1.5. Primary antibodies used in this study (Table 5).

Primary Abs	Host species	Dilutions	SOURCE	IDENTIFIER
SOX17	Goat	1:500	R&D systems	Cat#AF1924
GATA6	Goat	1:500	R&D systems	Cat#AF1700
ATP7B	Rabbit	1:5000	Abcam	Cat#ab124973
CP	Rabbit	1:300	Cell Signaling Technology	Cat#98971
Albumin	Goat	1:300	Bethyl	Cat#A80-229A
Alpha-Fetoprotein	Mouse	1:300	R&D systems	Cat#MAB1368
HNF4A	Mouse	1:300	R&D systems	Cat#MAB4605-SP
GAPDH	Mouse	1:500	R&D systems	Cat#MAB5718

NANOG	Rabbit	1:750	Reprocell	Cat#RCAB004P-F
OCT-3/4	Goat	1:500	R&D systems	Cat#AF1759-SP
OCT-3/4	Mouse	1:300	Santa Cruz	Cat#sc-5279
KLF4	Rabbit	1:750	MBL	Cat#PM057
SOX2	Mouse	1:500	R&D systems	Cat#MAB2018
SOX2	Goat	1:500	R&D systems	Cat#AF2018

### 3.1.6. Secondary antibodies used in this study (Table 6).

Secondary Abs	Dilution	SOURCE	IDENTIFIER
Donkey anti-Goat IgG (H+L) Highly Cross-Adsorbed Secondary Antibody, Alexa Fluor Plus 647	1:1000	Thermo Fisher Scientific	Cat#A32849
Alexa Fluor 555-conjugated goat anti- rabbit IgG	1:1000	Thermo Fisher Scientific	Cat#A21428
Donkey anti-Goat IgG (H+L) Highly Cross-Adsorbed Secondary Antibody, Alexa Fluor Plus 555	1:1000	Thermo Fisher Scientific	Cat#A32816
Donkey anti-Mouse IgG (H+L) Highly	1:1000	Thermo Fisher	Cat#A-31570

Cross-Adsorbed Secondary Antibody, Alexa Fluor 555		Scientific	
DyLight™ 649 Donkey anti-rabbit IgG	1:1000	Biolegend	Cat#406406

### 3.1.7. Chemicals used in this study (Table 7).

Chemical name	SOURCE	IDENTIFIER
PMA	Wako	Cat#183882
ATRA	Sigma-Aldrich	Cat#R2625
DAPT	Calbiochem	Cat#565784
CHIR99021	Wako	Cat#034-23103
PD0325901	Wako	Cat#162-25291
L(+)-Ascorbic Acid (L-AA)	Wako	Cat#012-04802
Dexamethathone	Nacalai tesque	Cat#11107-64
Y-27632	Wako	Cat#034-24024
A8301	Sigma-Aldrich	Cat#SML0788
Insulin	Nacalai tesque	Cat#12878-86

Forskolin	Nacalai tesque	Cat#16384-84
cis-4,7,10,13,16,19- Docosahexaenoic acid	Sigma-Aldrich	Cat#D2534
Bexarotene	Sigma-Aldrich	Cat#SML0282
Am80	Wako	Cat#017-16621
Tazarotene	Wako	Cat#517-87741

### 3.1.8. Reagents used in this study (Table 8).

REAGENT or RESOURCE	SOURCE	IDENTIFIER
iMatrix-511, silk (Laminin-511)	Nippi	Cat# 892021
StemFit™ StemFit AK02N medium	Ajinomoto	
CultureSure Y-27632	Wako	Cat#034-24024
Chromosome Analysis Suite	Thermo Fisher Scientific	
FastGene RNA premium kit	Nippon	Cat#FG-81250
ReverTra Ace qPCR RT kit	Toyobo	
Tks Gflex™ DNA Polymerase	Takara	Cat#R060A

FastGene™Gel/PCR extraction kit	Nippon	Cat#FG-91202
FastGene Plasmid Mini Kit	Nippon	Cat#FG-90502
THUNDERBIRD Probe qPCR Mix	Toyobo	Cat#QPS-101X5
StemSure DMEM	Wako	Cat#197-16275
L-alanyl-L-Glutamine solution	Nacalai Tesque	Cat#04260-64
0.5mol/l-EDTA Solution (pH 8.0)	Nacalai Tesque	Cat#06894-14
50 mM Monothioglycerol Solution	Wako	Cat#195-15791
MEM non-essential amino acids	Nacalai Tesque	Cat#06344-56
DMSO solution	Sigma-Aldrich	Cat#D2650 100ML
Penicillin (50U/ml 3uM)/Streptomycin (50ug/ml)	Nacalai Tesque	Cat#26252-94
DMEM/Ham's F12	Nacalai Tesque	Cat#11581-15
Stemsure serum replacement	Wako	Cat#191-18375
High efficiency DH5ALPHA Competent Cell	Gmbiolab	Cat#DH01-100
LB Broth, Miller	Nacalai Tesque	Cat#20068-75
LB Agar, Miller	Nacalai Tesque	Cat#20069-65

Mighty Cloning Reagent Set  (Blunt End)	Takara	Cat# 6027
B27 minus insulin	Thermo Fisher Scientific	Cat#A1895601
Recombinant human Oncostatin M	Wako	Cat#153-02101
Recombinant human Hepatocyte Growth Factor	Wako	Cat#082-08721
Activin A Solution, Human, recombinant	Wako	Cat#010-27623
Hepatocyte Basal Medium	Lonza	Cat#CC-3199
SDS-PAGE Sample Buffer Solution without 2-ME(2x) for SDS-PAGE	Nacalai Tesque	Cat#30567-12
Dithiothreitol (DTT)	Nacalai Tesque	Cat#14130-41
Protease inhibitor cocktail solution	Nacalai Tesque	Cat#04080-11
Pierce 660 nm Protein Assay Reagent	Thermo fisher	Cat#22662
Jes/Wes 12-230 kDa 8X25 capillaries cartridges separation module	ProteinSimple	Cat#SM-W004
Anti-Rabbit Detection Module for Jess, Wes, Peggy Sue or Sally Sue	ProteinSimple	Cat#DM-001
Anti-Mouse Detection Module for Jess, Wes, Peggy	ProteinSimple	Cat#DM-002

Sue or Sally Sue		
Anti-Goat Detection Module for Jess, Wes, Peggy Sue or Sally Sue	ProteinSimple	Cat#DM-003
STEM-CELLBANKER GMP Grade	Takara Bio	Cat# CB045
CellROX™ Deep Red Reagent	Thermo Fisher Scientific	Cat#C10491
Oleic acid	Sigma-Aldrich	Cat#O1383-1G
Lipi-Green reagent	DojinDo	Cat#LD02
96 well-V-plate	EZ-BindShut SP	Cat#4420-800SP
Guide-it™ Mutation Detection Kit	Takara	631448

### 3.2. Methods

#### 3.2.1. iPSCs generation and culture

HPS0045 (HiPS-RIKEN-5A), HPS0049 (HiPS-RIKEN-7A), and HPS0053 (HiPS-RIKEN-9A) iPSC lines were generated from skin fibroblasts deposited in RIKEN Cell Bank as RCB0395 NCU-F8, RCB0390 NCU-F3, and RCB0391 NCU-F4 obtained from 3 WD patients, respectively. These iPSC lines were reprogrammed with retroviral vectors carrying OCT3/4, SOX2, KLF4, and MYC,

according to the previous protocol[34]. HPS2807 WD iPSC line was generated from peripheral blood mononuclear cells obtained from a WD patient. This line was reprogrammed with episomal vectors carrying OCT3/4, SOX2, KLF4, MYCL1, Lin28, mp53DD, and EBNA1, according to the previous protocol[35]. Episomal vectors integration was inspired with EBNA-1 DNA copy number detection in the genome DNA of each iPSC line. All of these cell lines were deposited in RIKEN cell bank. The information detail of 4 patient iPSC lines were listed in the **Table 1**.

Feeder-free culture system was used to culture iPSC lines [36]. The iPSCs were cultured on 0.25  $\mu\text{g}/\text{cm}^2$  iMatrix-511 silk (Matrixome, Osaka, Japan) with StemFit AK02N medium (Ajinomoto). Cells were fed every other day and was passaged when reached 80–90% confluency after 6-8 days culture. 0.5 mM EDTA solution was used to dissociate cells into single cells, which was seeded in the density of 2500/ $\text{cm}^2$ . 10  $\mu\text{M}$  Y-27632 (Wako) was only used on the cell seeding day. All of the WD iPSC lines included in this study were identified as mycoplasma negative. STR (short tandem repeat) - PCR analysis was performed on all the iPSC lines to match the donor samples.

### **3.2.2. Microarray assay**

Copy number variations of WD iPSC lines were detected with a microarray assay using CytoScan Optima Suite (Thermo Fisher Scientific). CytoScan Optima

assay was performed according to the manufacturer's protocol. Before the assay, genomic DNA (gDNA) was extracted from WD-specific iPSCs with DNeasy Blood & Tissue Kit (Qiagen). The resulting CytoScan Optima arrays were read with GeneChip System 3000. Data were analyzed with Chromosome Analysis Suite (ChAS) and GeneChip Command Console Software (AGCC).

### **3.2.3. Pluripotency characterization with teratoma formation**

WD iPSCs were dissociated with 0.5 mM EDTA in D-PBS, then resuspended with 1 mL Stem Fit AK02N complete medium (Ajinomoto) supplemented with 10  $\mu$ M Y-27632 (Wako). Transfer cell suspension medium containing  $1 \times 10^6$  cells to a 1.5 mL tube. Cells were collected by centrifuged in 200 x g for 3 min and resuspended in Stem Fit AK02N complete medium (Ajinomoto) supplemented with 10  $\mu$ M Y-27632 containing 50% Matrigel solution. The cell suspension was aspirated in a 1 mL syringe with an 18G needle and kept on ice until injection. Cells were injected into the legs and testis of NOD.CB17-Prkdc<sup>scid</sup>/J, 4-week-old male mice,  $1 \times 10^6$  cells per injection (Charles River Laboratories JAPAN, Inc. <https://www.crl.co.jp/>). Six to ten weeks later, teratomas were collected from legs or testis, and fixed with 4% paraformaldehyde dissolved in D-PBS (Nacalai Tesque) for 1 week at 4°C, and further stored with 70% ETOH at 4°C for weeks. Paraffin-embedded sections were made by Genostaff inc. and processed for haematoxylin and eosin (HE) staining. Three germ layers derived derivatives were observed by BZ-X800 microscope (KEYENCE). All mice used in this study

were bred and euthanized appropriately, following ethics of animal research committee in RIKEN.

#### **3.2.4. Pluripotency identification with embryonic body formation**

WD iPSC lines were prepared as above.  $1.0 \times 10^4$  cells were seeded in 96-well-V plate (EZ-BindShut) in each well with 100uL Stem Fit AK02N complete medium (Ajinomoto) supplemented with 10  $\mu$ M Y-27632 (Wako). Cells were centrifuged at 200g, 3 min before culture. The next day, the culture medium was changed into DMEM high Glucose (Gibco) supplemented with 10% fetal bovine serum (EB medium), 100 uL per well. Seven days later, EBs were transferred into 0.1 w/v% Gelatin Solution (WAKO)-coated 24-well plate and further cultured in EB medium for another 7 days. Cells were fed every other day. Pluripotency was validated by checking three germ layer markers (TUJ1/SMA/AFP) expression with immunostaining.

#### **3.2.5. Mutation identification in WD-Hep**

To identify the ATP7B mutations in each WD iPSC line, WD patient iPSC derived hepatocytes were collected around day 17 and total RNA were extracted with FastGene RNA premium kit (Nippon Genetics). cDNA was synthesized by reverse transcription (RT) kit. Less than 1 ug mRNA was further used for the first-

strand cDNA synthesis using ReverTra Ace qPCR RT kit (Toyobo). To synthesis the whole length transcript of ATP7B gene, oligo dT was used in the RT reaction. Thermal condition for RT reaction was as follows, 30°C, 10 minutes, 42°C; 60 minutes; 99°C, 5 minutes. Ten pairs of primers were designed based on transcript variant 1 (GenBank Accession Number: NM\_000053.4), which were used to amplify the whole coding sequence of ATP7B with Tks Gflex DNA Polymerase (Takara). Primer sequences were listed in **Table 2**. The thermal cycling conditions were as follow: initial denaturation at 94 °C for 1 min, 35 cycles of 3-step thermo-cycling (denaturation at 98 °C for 10 s, annealing at 60 °C for 15 s and extension at 68 °C 60 s), then hold at 4 °C. PCR products were confirmed by agarose gel electrophoresis before sequence analysis. PCR products used for sequence were prepared with FastGene Gel/PCR extraction kit (Nippon Genetics).

Mutations in each WD iPSC line were further verified in the respective genomic DNA sample. Genomic DNA was prepared using DNeasyBlood & Tissue Kit (Qiagen). PCR primer sequences used for ATP7B genome sequence are listed in **Table 3**. Thermal cycling conditions were the same as above. All the experiments were performed following the manufacturer's instructions of the respective kit. Sanger sequence analysis was further performed with Genetic Analyzer 3130 (Applied Biosystems) to identify the mutations on each fragment.

### **3.2.6. TA-cloning**

To clarify the allelic location of these heterozygous mutations in each WD iPSC lines, the Cloning Reagent Set (Blunt End) (Takara) was used to clone the targeted PCR fragments into pUC118Hinc II/BAP, a blunt-end cloning vector containing a multiple cloning site, then followed by a credible blue/white colony selection. New plasmid was constructed by ligation reaction between pUC118 and interested PCR product, which were further transformed into E. coli DH5-a, by incubated with competent cells for 30min at 4°C, then shocked at 42°C for 45 seconds, further recovered by putting on ice 4°C for 2 minutes. After 1 hour shaking culture at 280 rpm in SOC medium at 37 °C, the transformed E. coli was spread on LB agar (Nacalai tesque) plate and incubated at 37°C overnight. Single colonies were picked up and incubated in 3 ml LB medium (Nacalai tesque) at 280 rpm for 8 hours. Plasmids were prepared with miniprep plasmid extraction kit (FastGene Plasmid Mini Kit). Plasmid concentration was determined by Nanodrop. All the experiments were performed following the manufacturer's instructions of the respective kit. The cloned inserts were sequenced through PCR by using M13 primer FW (20): GTAAAACGACGGCCAGT, and M13 primer RV: CAGGA AACAG CTATG AC in Fasmac or Eurofin companies.

### **3.2.7. Quantitative RT-PCR**

Total RNA preparation and first-strand cDNA synthesis protocol were the same as above. Random primer was used for first-strand cDNA synthesis, instead of oligo dT. Real-Time qPCR reactions were performed on QuantStudio 3 System (Applied Biosystems) using THUNDERBIRD Probe qPCR Mix (Toyobo) with TaqMan probes according to manufacturer's instructions. The respective genes expression level was shown as fold change relative to the value of control sample ( $\Delta\Delta C_t$  method) after normalized to corresponding GAPDH values. TaqMan probes used for RT-qPCR experiments were listed in **Table 4**.

### **3.2.8. Immunostaining**

Immunostaining was performed to check the expression of pluripotency markers (OCT4/NANOG/SOX2/KLF4), endoderm related markers (SOX17/GATA6) and hepatocyte related markers expression (HNF4A/AFP/ALB). Briefly, cells were fixed with PBS containing 4% paraformaldehyde for 10 min at room temperature. For staining transcription factors, cells were permeabilized in PBS containing 0.1% Triton X-100 for another 10 minutes at room temperature, then washed with PBS. Primary antibodies were incubated in 0.1% FBS in PBS overnight at 4°C. Primary Abs used in this study were listed as **Table 5**. Secondary antibodies were incubated for 1 hour at room temperature in 0.1% BSA in PBS. Secondary antibodies used in this study were listed in **Table 6**. Cell nuclei were stained with Fluoro-KEEPER Antifade Reagent DAPI (Nacalai Tesque). Images were taken with all-in-one fluorescent microscope (KEYENCE, BZ-X800).

### 3.2.9. Hepatocyte differentiation

Three stages differentiation protocol was adopted to differentiate iPSC into hepatocyte in this study (modified from Siller et al., Stem Cell Reports 2015). For differentiation preparation, iPSC was dissociated with 0.5 mM EDTA in PBS, and then  $2.5 \times 10^4$  iPSC were seeded in each well of a 24-well plate with StemFit complete culture medium (Ajinomoto) supplemented with 10  $\mu$ M Y-27632 (Wako) and 0.25  $\mu$ g/cm<sup>2</sup> iMatrix-511 silk (Matrixome) at on day 0. The first stage was from day 1 to day 2. To initiate differentiation, the culture medium was changed to StemFit (without supplement C) supplemented with 3  $\mu$ M CHIR99021 (Wako) and 10 ng/ml Activin A (Wako) on day 1. The culture medium was changed into StemFit (without supplement C) on day 2. The second stage was from day 3 to day 7. During this stage, cells were cultured in StemSure DMEM (Wako) supplemented with 20% Stemsure serum replacement (Wako), 1% L-alanyl-L-Glutamine solution (Nacalai Tesque), 1% 50 mM Monothioglycerol Solution (Wako), 1% MEM non-essential amino acids (Nacalai Tesque), 1% DMSO solution (Sigma Aldrich), 1% Penicillin (50 U/ml 3 uM)/Streptomycin (50  $\mu$ g/ml) (Nacalai Tesque), 5  $\mu$ M DAPT (Calbiochem) and 0.3  $\mu$ M A83-01 (SIGMA). The culture medium was changed every other day. The third stage was from day 7 to day 17. During this stage, cells were cultured in DMEM/Ham's F12 (Wako) supplemented with 1% Stemsure serum replacement (Wako), 1% L-alanyl-L-Glutamine solution (Nacalai Tesque), B27 minus insulin (Gibco), 1% MEM non-

essential amino acids (Nacalai Tesque), 1% Penicillin (50 U/ml 3 uM)/Streptomycin (50 ug/ml) (Nacalai Tesque), 10 ng/ml recombinant human Hepatocyte Growth Factor (rhHGF) (Wako) and 10 ng/ml recombinant human Oncostatin M (rhOSM) (Wako), 5 uM DAPT (Calbiochem), 0.3 uM A83-01 (SIGMA) and Dexamethasone (10 uM) (Nacalai Tesque), the culture medium was changed every other day. On day 15, cells were washed with D-PBS for twice, and the culture medium was changed into Hepatocyte Basal Medium (Lonza) supplemented with 20 ng/ml rhHGF (Wako), 20 ng/ml rhOSM (Wako) 1% Penicillin (50 U/ml 3 uM)/Streptomycin (50 ug/ml) (Nacalai Tesque).

### **3.2.10. Cell lysate and culture supernatant preparation for Simple Wes**

To detect ATP7B protein, day 17 of iPSC-derived hepatocytes were collected. The cell lysate was prepared with SDS-PAGE Sample Buffer Solution without 2-ME (2x) (Nacalai Tesque) supplemented with 10% 1 M Dithiothreitol (DTT) solution (Nacalai Tesque) and 1% protease inhibitor cocktail solution (Nacalai Tesque). To detect secreted Ceruloplasmin (Cp), cell culture supernatant was collected from day 17 of iPSC-derived hepatocyte, then centrifuged at 6000 rpm, 3 min. Protein concentration was determined with Pierce 660 nm Protein Assay Reagent (Thermo Scientific) and a rainbow sunrise microplate reader (TECAN).

### 3.2.11. Automatic capillary western blot

Western blotting was performed with capillary automatic western blot device (Simple western, Wes). For total Albumin, ATP7B and total Cp detection, Jes/Wes 12-230 kDa 8X25 capillaries cartridges separation module (ProteinSimple) was used for protein separation. Anti-Rabbit/Goat/Mouse Detection Module kit (ProteinSimple) for Wes was used for protein detection. Sample loading and reagent preparation were all conducted following the manufacturer's instructions. For the supernatant, around 10 µg of total protein amount was loaded to each well. For the cell lysate, around 3 µg of total protein amount was loaded to each well. For pre-loading preparation, samples were diluted with Simple Western 0.1 x sample dilution buffer then mixed with 1/5 volume Fluorescent Standards Mix containing DTT, then denatured at 95 °C for 5 min. The following primary antibodies were used to blot the target protein, anti-GAPDH, anti-ATP7B, anti-Human Albumin, and anti-Ceruloplasmin. Detailed information of the primary antibodies is listed in **Table 5**.

Chemiluminescent signal was detected and quantitated by Simple Western system automatically. Compass Software was used to process and analyze the data. The area of blot bands was quantified as its protein expression level. To normalize ATP7B, ALB, AFP, CK7, CK19 expression level in the same sample, one of the housekeep protein, GAPDH, was used as the reference. To normalize Cp secretion level in different samples, secreted ALBUMIN protein was used as the reference.

### 3.2.12. Cp secretion-based drug screening

Some chemicals were used for the candidates to increase Cp secretion level in WD-specific iPSC-derived hepatocytes. Included chemicals were as follows: PMA, all-trans retinoic acid, DAPT, CHIR99021, PD0325901, L(+)-Ascorbic Acid (L-AA), Dexamethasone, Y-27632, A8301, Insulin, Forskolin. All of these drugs were administered to the cells at a concentration of 1  $\mu$ M. Drug treatment was started from differentiation day 13. To get rid of the effect of serum and undefined factors, hepatocyte cultures were washed with D-PBS twice before being changed into drug screening culture medium on day 13, which comprised of HBM (Lonza) supplemented with rhHGF (Wako) 20 ng/ml and rhOSM (Wako) 20 ng/ml containing the respective drugs. Cells were fed once with the same medium and drugs on day 15. On differentiation day 17, cell culture supernatants were collected for examining secreted Cp and Albumin of each culture condition with the automatic capillary western blot device described above.

Two RXRs selective agonists (Bexarotene and cis-4,7,10,13,16,19-Docosahexaenoic acid) and RARs selective agonists (Tazarotene and Am80) treatment and sample collecting protocol were same as above. Information for chemicals used in this paper is listed in **Table 7**.

### **3.2.13. Oleic acid exposure and retinoids, RXR/RARs agonists treatment**

Oleic acid exposure was started from differentiation day 11-day 13 for about one week. Cells were cultured in the third stage differentiation medium containing OA (0, 50, 100, and 200  $\mu$ M) (SIGMA). To test the inhibitory function of ATRA and RXR/RARs agonists on reactive oxygen species (ROS) production, ATRA and the indicated agonists were added for the last 4 days before sampling. CellROX Deep Red Reagent (Thermo Scientific) and Lipi-Green reagent (DojinDo) were used to detect the production of ROS and lipid droplets in WD-Hep, respectively. ROS production and lipid droplet in hepatocyte were visualized with an all-in-one fluorescent microscope (KEYENCE, BZ-X800). Cell nuclei were stained with Fluoro-KEEPER Antifade Reagent DAPI (Nacalai Tesque). Tiled whole-well fluorescent images were taken for ROS production as well as lipid accumulation level evaluation. The integrated density (Intden) of the entire well fluorescence was measured by the software of Image J 1.53.e after the background subtraction. To normalize ROS production and lipid accumulation level in different wells, the Intden of DAPI in the entire well was used as the reference.

### **3.2.14. RNA-Seq**

Total RNA of 12 samples was extracted with FastGene RNA premium kit (Nippon Genetics). Strand-specific library preparation was performed. The prepared

library was sequenced by NovasSeq6000 (Illumina). Sequencing was performed in a 2x150 bp PE configuration with a data output of about 6 Gb per sample (equivalent to about 20 million paired reads). The quality score (Q30) of all the sample were more than 94%. Library preparation and sequencing were performed in GENEWIZ. The sequencing data was analyzed with CLC genomics workbench (QIAGEN) to identify differentially-regulated genes and to draw a volcano plot. The extracted genes were analyzed for enrichment in gene ontology and biological pathways in Enrichr web program (<https://maayanlab.cloud/Enrichr/>).

## 4. Results

### 4.1. Generation and characterization of four WD patient-derived iPSCs

In this study, I used four WD iPSC lines generated from the patients suffered from WD by CiRA and RIKEN cell bank, namely HPS0045, HPS0049, HPS0053, and HPS2807, of which HPS0045, HPS0049, HPS0053 were generated by retroviral vectors and HPS2807 were generated by non-integrating episomal DNA vectors (**Table 1**). The pluripotency of four WD iPSC lines was examined with different methods. Firstly, the pluripotency markers expression by these four WD iPSC lines was examined with immunochemistry. The results showed that all of these 4 WD-iPSC lines highly expressed self-renewal markers of iPSCs, such as OCT3/4, NANOG, SOX2 and KLF4 (**Fig. 1A and B**).

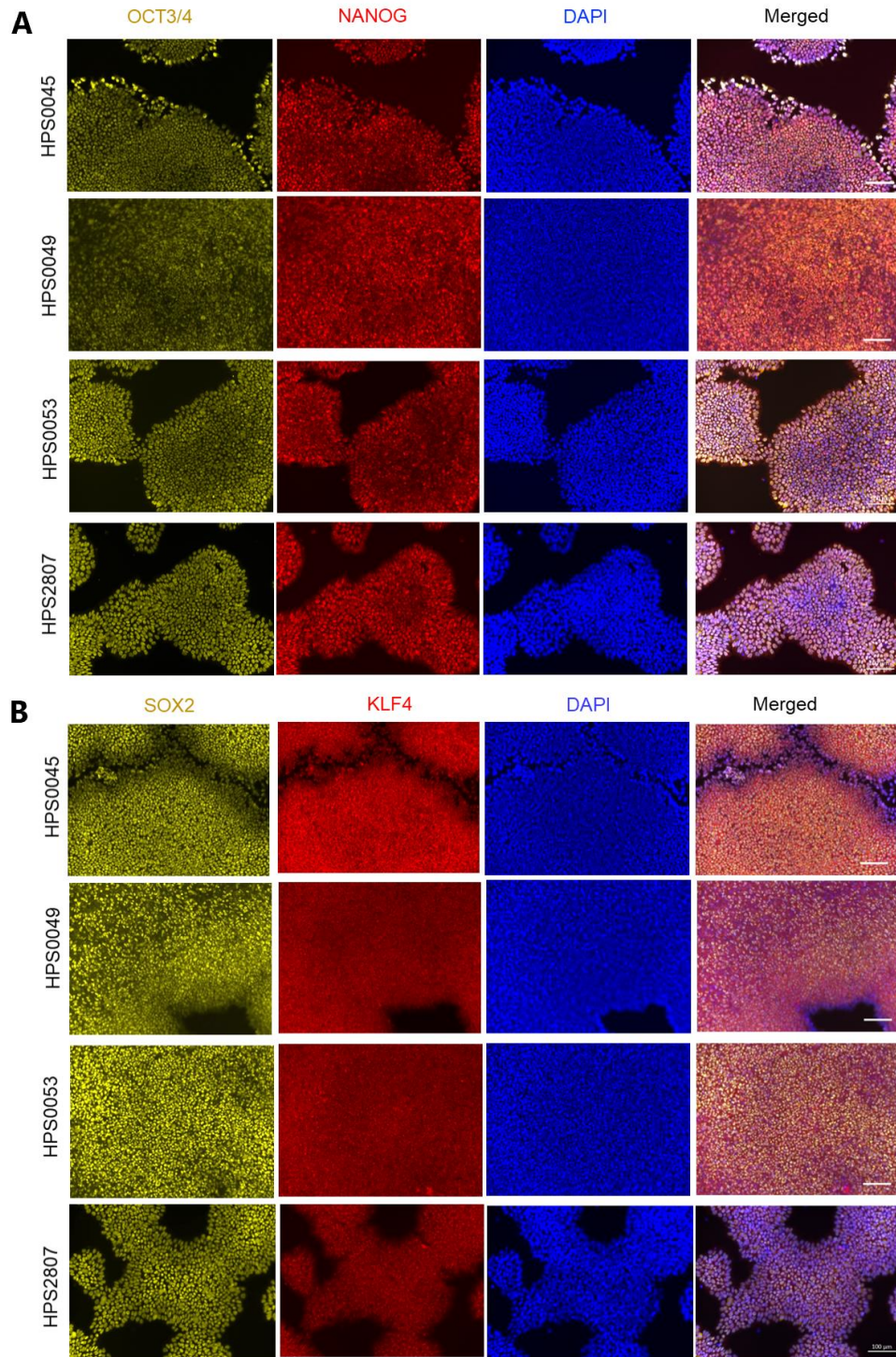


**Figure 1. Pluripotency markers expression of four WD iPSC lines. A and B.** Immunostaining results showing OCT3/4 and NANOG (A), SOX2 and KLF4 (B) protein expression in four WD iPSC lines. Scale bar is 100  $\mu$ m.

Secondly, embryoid body (EB) formation assay which allowed spontaneous differentiation of iPSCs into three germ layers *in vitro* was used to examine the multiple differentiation capacity of these four WD iPSC lines. The results showed the three-germ layer related markers can be detected in the EB from 4 WD iPSC lines (**Fig. 2A**). It indicated the pluripotency of 4 WD-iPSC lines. Thirdly, teratomas formation experiment were further used to examine the pluripotency of 4 WD iPSC. The results showed that the teratoma from these four WD iPSC lines were containing various tissues derived from three germ layers (**Fig. 2B**).

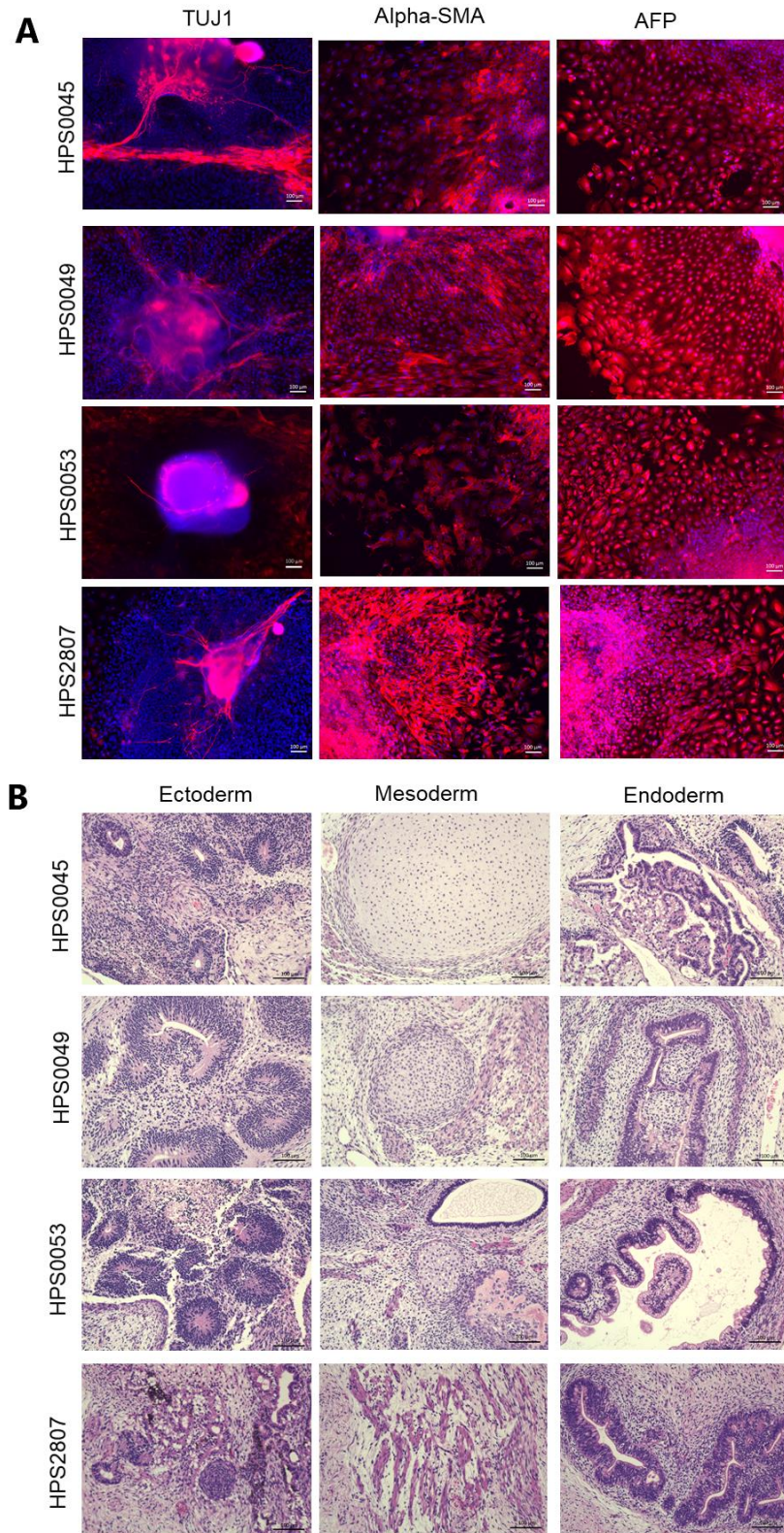


**Figure 2. Pluripotency characterization of four WD iPSC with EB formation and teratoma formation assay. A.** Three germ layer markers expression in four WD iPSC lines derived

embryoid body (EB) detected by Immunostaining. TUJ1, alpha-SMA and AFP were used as ectoderm, mesoderm and endoderm markers, respectively. **B.** Three germ layer derivatives of four WD iPSC lines derived teratoma. The neuronal structure (HPS0045, HPS0049 and HPS0053) and melanocyte like structures (HPS2807) representing the ectoderm derivatives. Cartridge structure (HPS0045, HPS0049 and HPS0053) and smooth muscle structures (HPS2807) representing the mesoderm derivatives. Gastrointestinal structure representing the endoderm derivatives. Scale bar is 100  $\mu\text{m}$ .

To examine the chromosome integrity, comparative genome hybridization (CGH) array analysis was performed. The results showed all of these WD-iPSC lines had normal karyotype without large copy number variations (**Fig. 3**). It indicated the safety for the clinical application and genetic stability of these four iPSC lines. Collectively, our characterization results indicated that these WD-iPSC lines maintained self-renewal, pluripotency, genomic integrity.

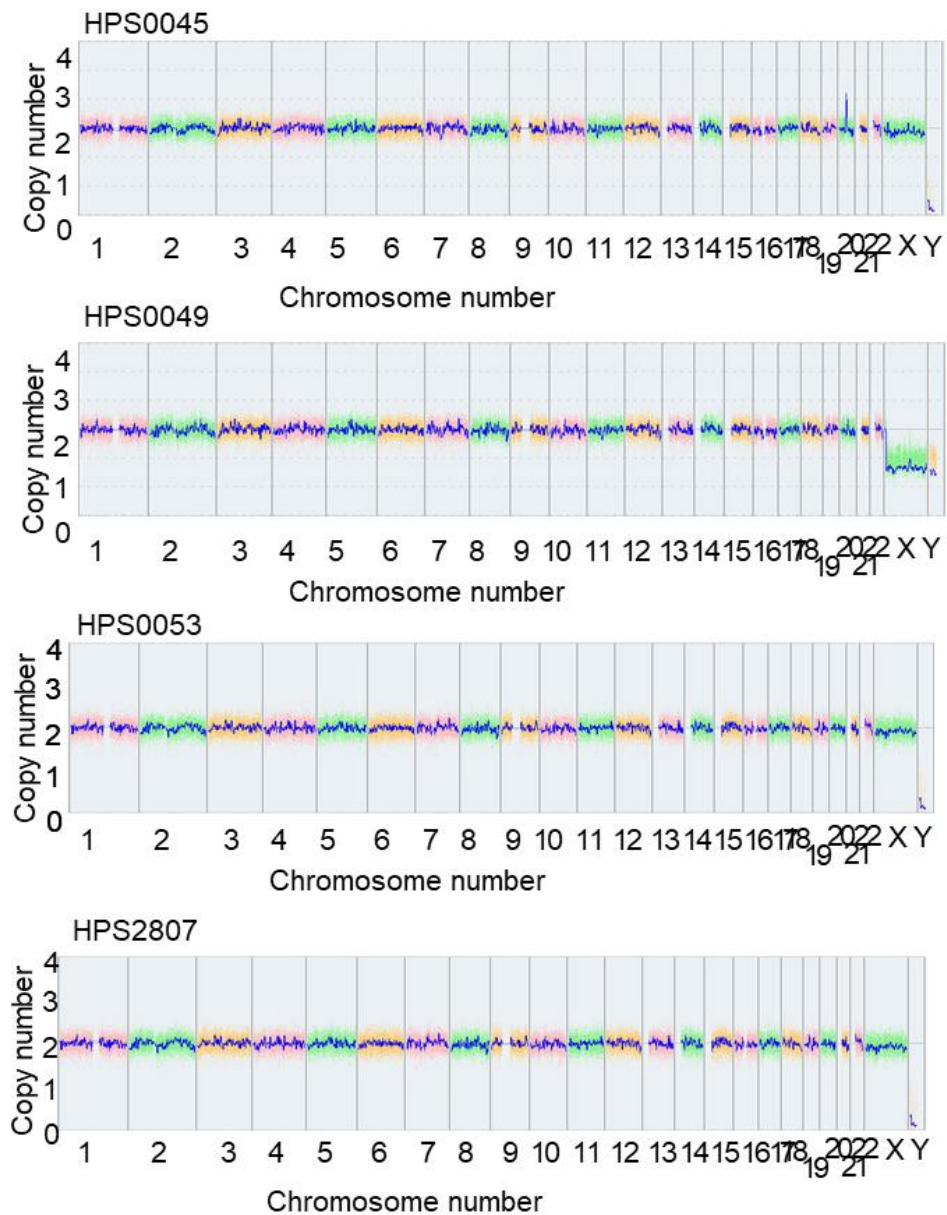


**Figure 3. Comparative genome hybridization (CGH) array of four WD iPSC lines.**

#### **4.2. ATP7B mutation identification in four WD iPSCs**

As *ATP7B* was the responsible gene of WD [37, 38], the mutations in this gene carried by four WD-iPSC lines were detected by sequencing the entire coding region of *ATP7B*

from cDNA in WD-iPSC-derived hepatocyte cultures. The entire coding region of ATP7B from cDNA was amplified with 10 pairs primers. The results were further verified in the genomic DNA of these WD-iPSCs. The relative allelic localization was further identified with TA cloning. Collectively, the sequence results showed that HPS0045 iPSC line carried R778L (c.2333G>T), K832R (c.2495A>G) and R952K (c.2855G>A) heterozygous mutations (**Fig.4A**). HPS0049 and HPS0053 iPSC lines were carrying two same mutations, which were G1035V (c.3104G>T) and V1262F (c.3784G>T) heterozygous mutations. Here I need to mention that these two patients were siblings (**Fig. 4B**). HPS2807 iPSC line carried S406A (c.1216T>G), V456L (c.1366G>C), K832R (c.2495A>G), R952K (c.2855G>A), P992L (c.2975C>T) and K1010T (c.3029A>C) heterozygous mutations. Among them, the relative allelic location of S406A (c.1216T>G), V456L (c.1366G>C) were not clear, because their location is too far from other mutations sites which is difficult to be detected by TA-cloning method. (**Fig. 4C**). All of the heterozygous mutations identified in these four WD iPSC lines were distributed on different alleles which indicated that these mutations could affect all of the expressed protein in the respective cell line. In this case, the mutations carried by all of these four WD iPSC lines were defined as compound heterozygous mutations.

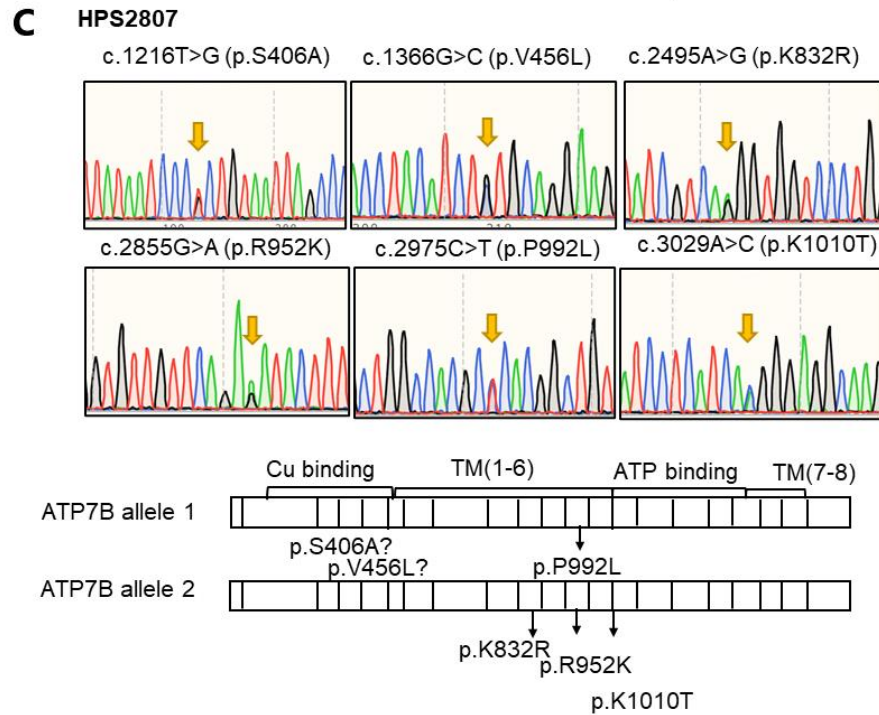
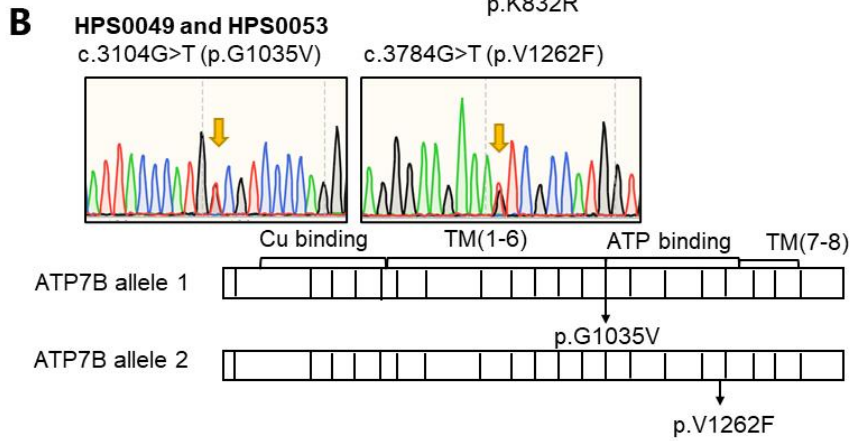
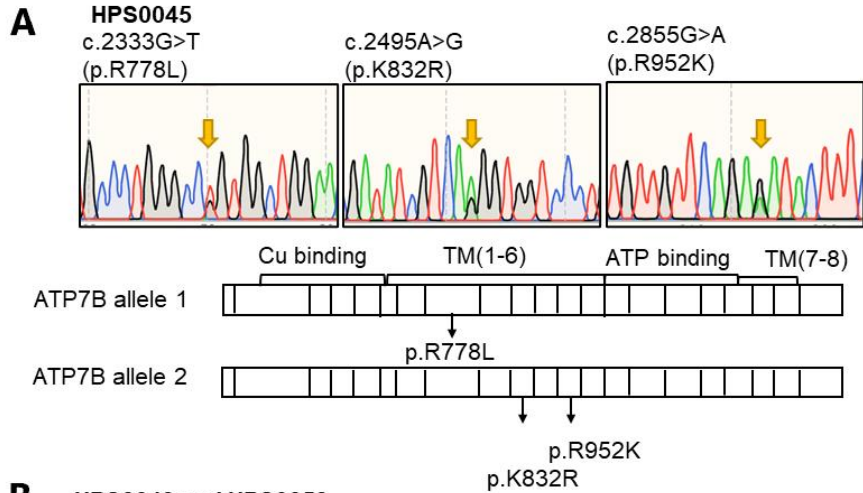
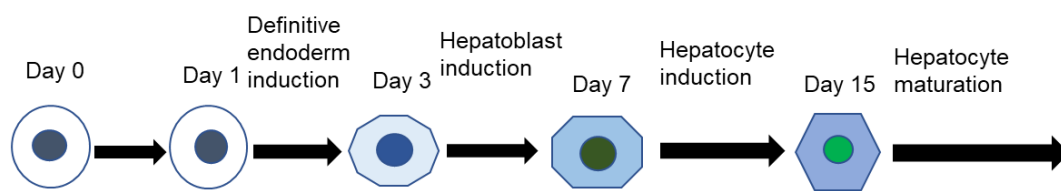


**Figure 4. ATP7B mutations carried by four WD iPSC lines.** Mutations and allelic locations were shown as the illustration. HPS0045(A), HPS0049 and 0053(B), HPS2807(C).

### 4.3. Hepatic differentiation of WTC11 iPSC line

For WD disease modeling with WD iPSC lines *in vitro*, a hepatic differentiation protocol was established which was modified from a protocol reported in a previous study [39]. An iPSC line from a healthy donor (i.e., WTC11 line (GM25256)) were differentiated into hepatocytes under this differentiation protocol (**Fig. 5**). With this protocol, cells could highly express definitive endodermal marker genes, *SOX17* and hepatic markers, such as *HNF4A* and *DLK1*, on day 4-7 (**Fig. 6A**). Hepatocyte marker genes, alpha-fetoprotein (*AFP*), albumin (*ALB*) and alpha-1-antitrypsin (*A1AT*) got highly expression on day 17 (**Fig. 6B**). Immunostaining was performed to examine these markers protein expression. Results showed that there was a high percentage cells expressing definitive endodermal marker proteins, *SOX17* and *GATA6*, on day 5 (**Fig. 6C and D**). The hepatic marker proteins, such as *HNF4A*, *AFP*, and *ALB*, were highly expressed on day 17 (**Fig. 6E-G**).



Medium name	Maintenance medium	Definitive endoderm induction medium	Hepatoblast induction medium	Hepatocyte induction medium	Hepatocyte maturation medium
Basal medium	StemFit AK02N	StemFit AK02N	Stemsure DMEM	DMEM/F12	HBM
Additives	Supplement B, Supplement C, 10 $\mu$ M Y-27632, 0.25 $\mu$ g/cm <sup>2</sup> iMatrix-511 silk	Supplement B <u>Only on day 1</u> 3 $\mu$ M CHIR99021, 10 ng/ml Activin A	20% SSR, 1% NEAA, 1% Glutamax, 1% MTG, 1% DMSO, 5 $\mu$ M DAPT, 0.3 $\mu$ M A83-01, 1% P/S	1% SSR, 2% B27 minus insulin, 20 ng/ml HGF, 20 ng/ml OSM, 10 $\mu$ M Dexamethasone, 5 $\mu$ M DAPT, 0.3 $\mu$ M A83-01, 1% P/S	20 ng/ml HGF, 20 ng/ml Oncostatin M, 10 $\mu$ M Dexamethasone, 5 $\mu$ M DAPT, 0.3 $\mu$ M A83-01, 1% P/S

**Figure 5. Hepatocyte differentiation protocol.** Schema of hepatocyte differentiation from iPSC.

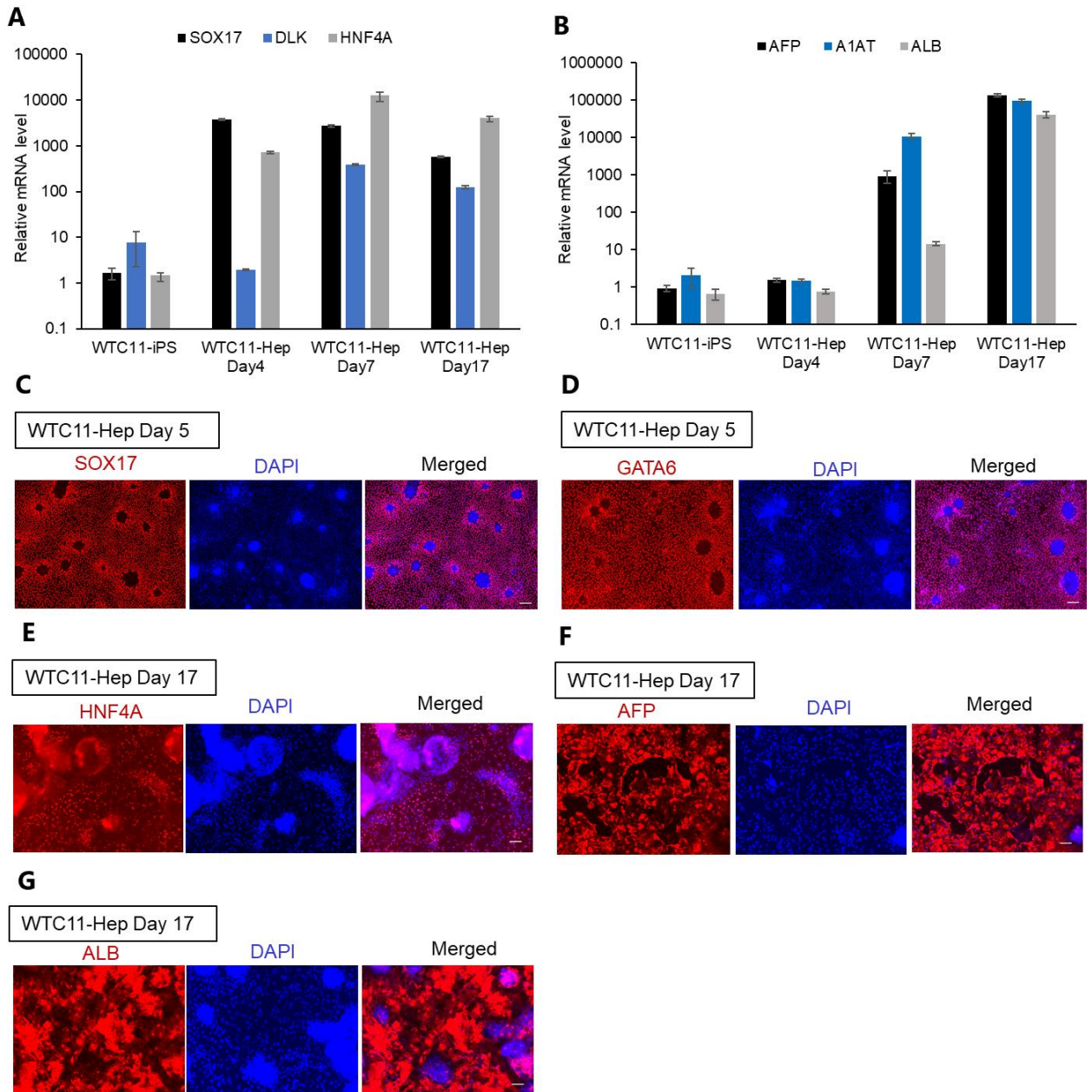


**Figure 6. Hepatocyte differentiation of WTC11 iPSC.** **A** and **B.** RT-qPCR results showing SOX17, DLK and HNF4A gene (**A**) expression and AFP, A1AT and ALB gene (**B**) expression on day 4, 7 and 17. **C** and **D.** Representative immunostaining images showing SOX17 (**C**) and GATA6 (**D**) protein expression on differentiation day 5. **E-G.** Representative immunostaining images showing HNF4A (**E**), AFP (**F**) and ALB (**G**) on differentiation day 17. Scale bar is 100  $\mu$ m.

#### **4.4. Hepatic differentiation and characterization of WD iPSCs**

WD iPSC lines were differentiated into hepatocyte under above protocol. Hepatic differentiation capacity of WD iPSC were evaluated by comparing the hepatic markers gene expression (AFP and A1AT) between WD iPSC line derived hepatocytes (WD-Hep) and WTC11 iPSC line derived hepatocyte (WTC11-Hep). RT-qPCR results showed that WD-Hep expressed comparable levels of these two hepatic marker genes as WTC11-Hep (**Fig. 7A-D**).

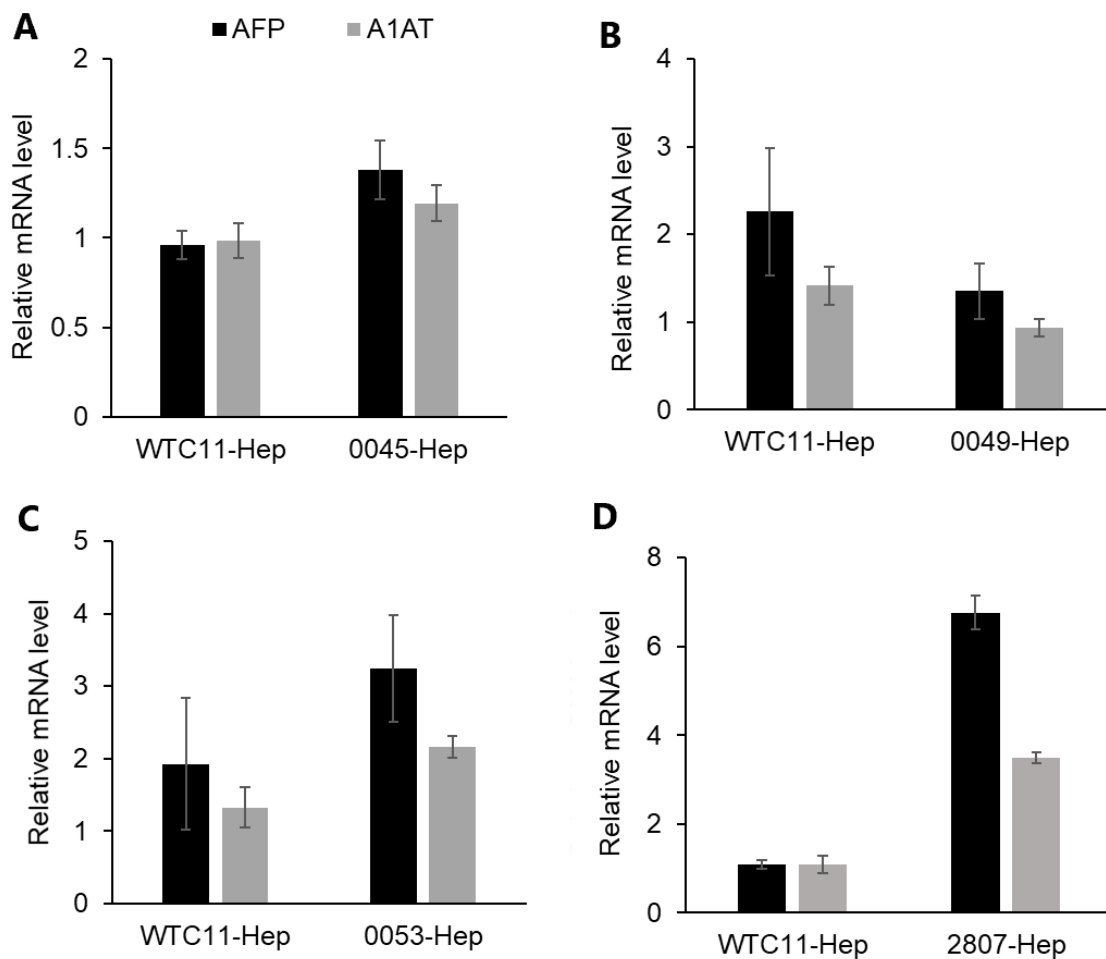


**Figure 7. Comparison of hepatic differentiation capacity between WD specific hepatocyte and WT iPSC derived Hepatocyte.** A-D. RT-qPCR results showing the AFP and A1AT mRNA expression in the indicated WD iPSC line derived Hepatocyte relative to WTC11 iPSC derived Hepatocyte. Bar graphs show the mean  $\pm$  SEM (n=3).

Hepatic related proteins (HNF4A/AFP/ALB) expression was further examined with immunochemistry. The results showed that WD-specific hepatocyte could express similar level of three hepatic proteins as WTC11 iPSC derived hepatocyte on differentiation day 17 (**Fig. 8A-C**). These results indicated WD-specific iPSCs possessed the comparable hepatic differentiation ability with

WTC11 iPSCs. It suggested that the suitability of my present hepatic differentiation protocol for WD modeling *in vitro*.

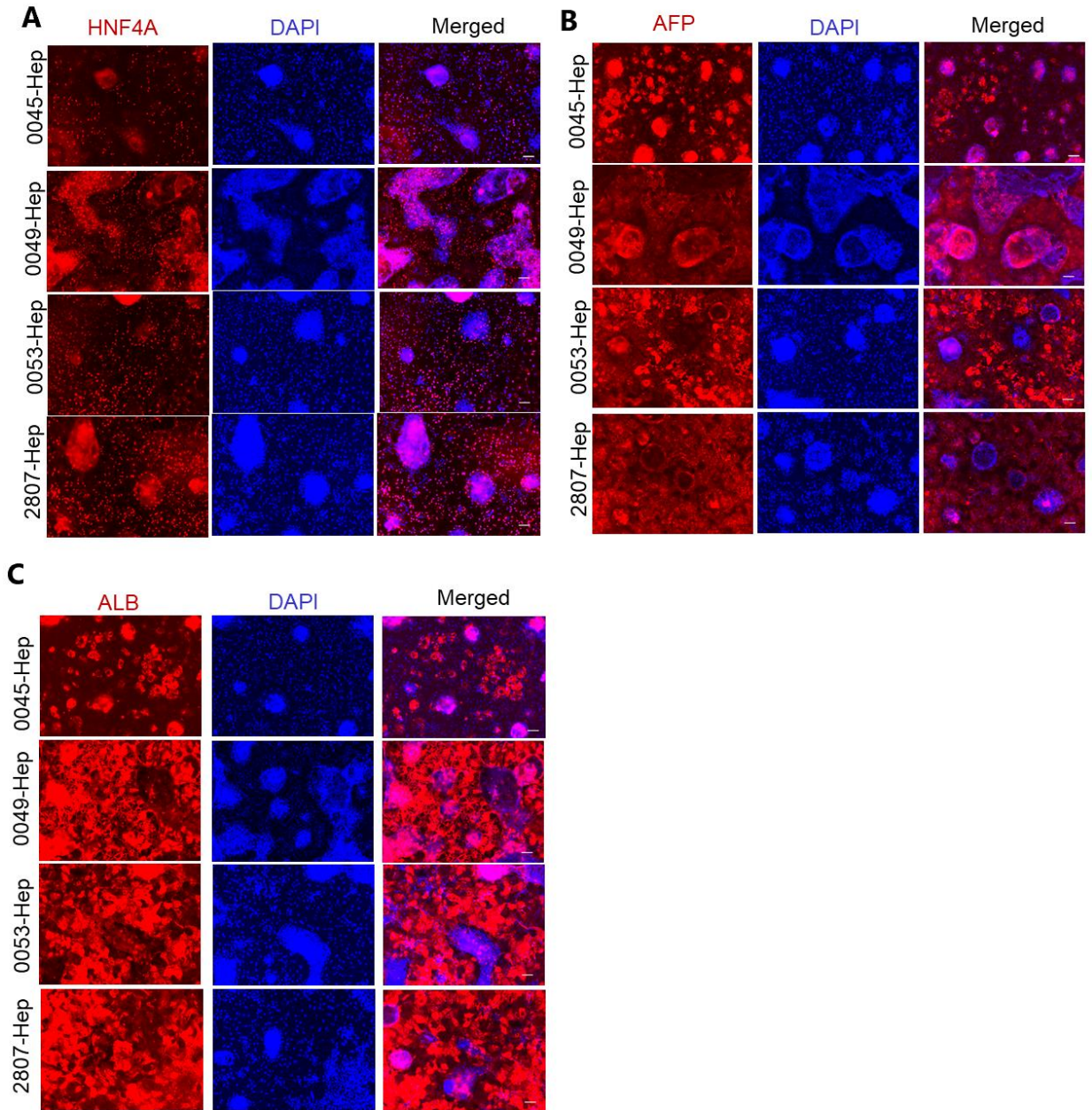


**Figure 8. Hepatic markers detection in four WD iPSCs derived hepatocyte. A-C.**

Representative immunostaining images showing HNF4A(A), AFP(B) and ALB(C) protein

expression in four WD iPSC lines derived hepatocyte on differentiation day 17. Nuclear were co-stained with DAPI. Scale bar is 100  $\mu\text{m}$ .

#### **4.5. ATP7B expression in four WD iPSC lines derived hepatocytes**

To identify how WD mutations affected ATP7B expression, I further examined the mRNA and protein expression level in WD iPSC-derived hepatocytes. From the result of WTC11 iPSC derived hepatocyte, I found that *ATP7B* mRNA expression level constantly increased under this differentiation protocol (**Fig. 9**). Further, the expression levels of ATP7B mRNA and protein of WD-specific hepatocytes were examined on differentiation day 17 with RT-qPCR and western blot, respectively. The RT-qPCR results showed that all the WD specific hepatocyte expressed a comparable level of *ATP7B* mRNA with WTC11 iPSC derived hepatocyte (**Fig. 10A-D**). It suggested the mutations carried by the four WD iPSC has no obvious effects on the mRNA expression of ATP7B gene.

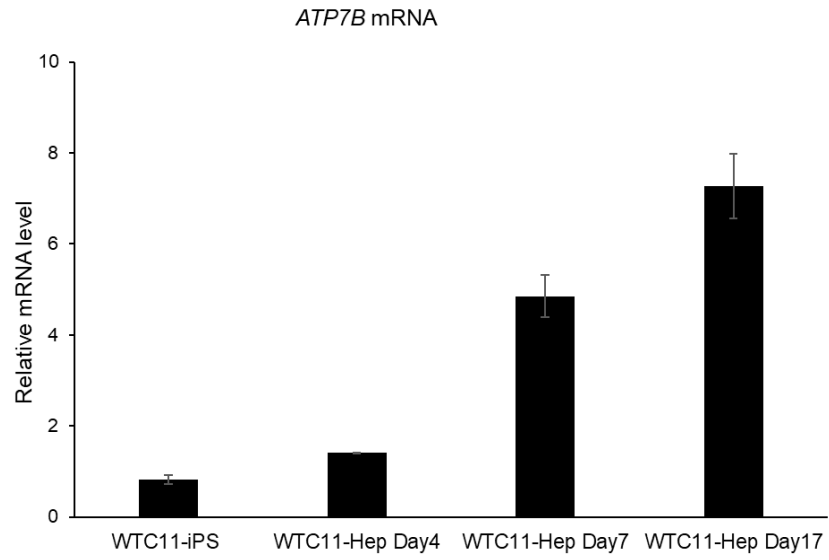


**Figure 9. ATP7B mRNA expression in WD iPSC derived Hepatocyte.** RT-qPCR result showing ATP7B mRNA expression on differentiation day 4, 7 and 17 of WTC11 iPSC. Bar graphs show mean  $\pm$  SEM (n=3).

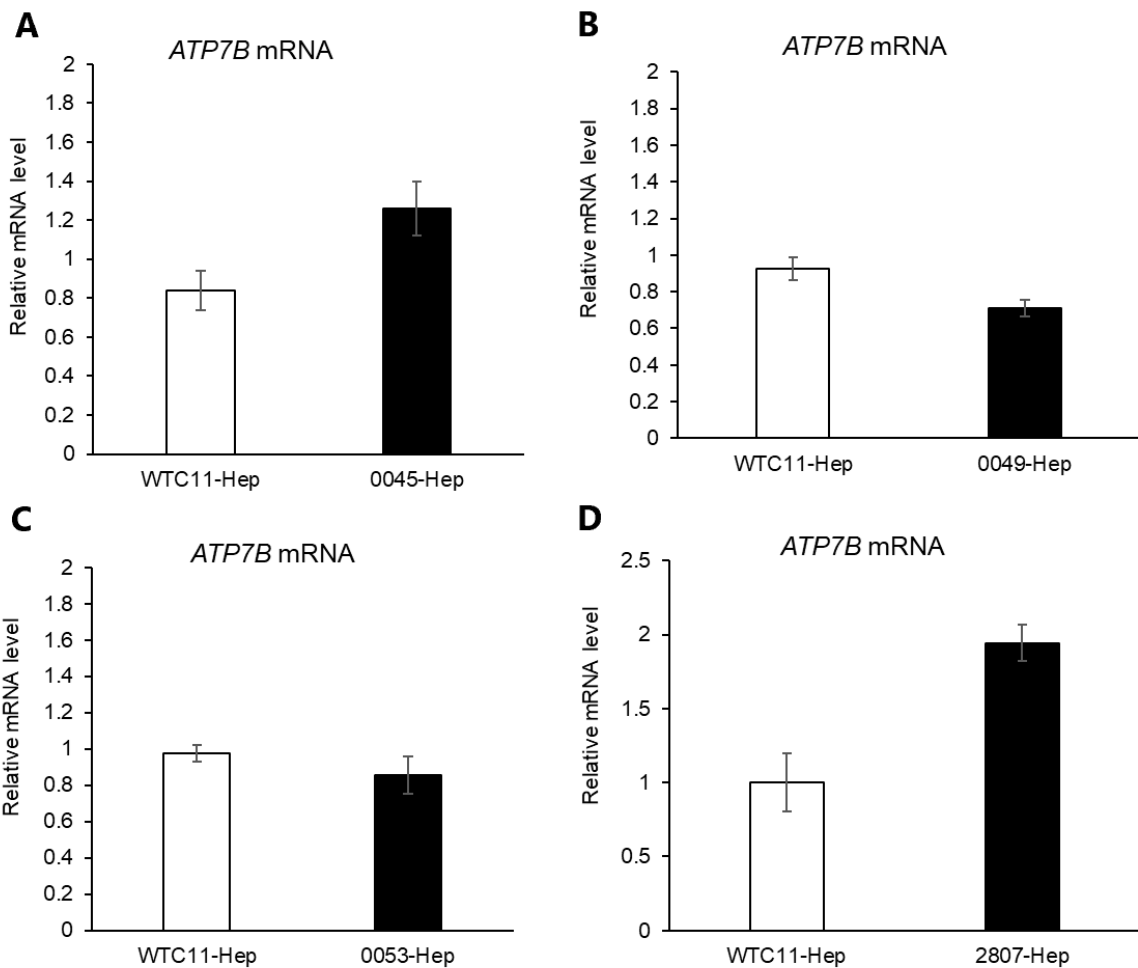


**Figure 10. Comparison of ATP7B mRNA expression between WD-specific hepatocyte and WT iPSC derived hepatocyte. A-D.** RT-qPCR result showing ATP7B mRNA expression in the indicated WD specific hepatocyte relative to WTC11 iPSC derived hepatocyte on differentiation day 17. Bar graphs show mean  $\pm$  SEM (n=3).

The western blot results showed that HPS0045-derived hepatocytes expressed the lower (but not a significant) amount of ATP7B protein comparing with the WTC11 iPSC derived hepatocyte (**Fig. 11A and B**); HPS0049- and HPS0053-derived hepatocytes expressed almost no ATP7B protein (**Fig. 11C-E**); HPS2807-derived hepatocytes expressed a similar amount of ATP7B protein

compared to WTC11-derived hepatocytes (**Fig. 11F-G**); These results suggested that WD-specific iPSC-derived hepatocytes expressed highly variable levels of ATP7B protein. It implied that the effects of these mutations on the ATP7B protein might be via post-transcriptional regulation processes.

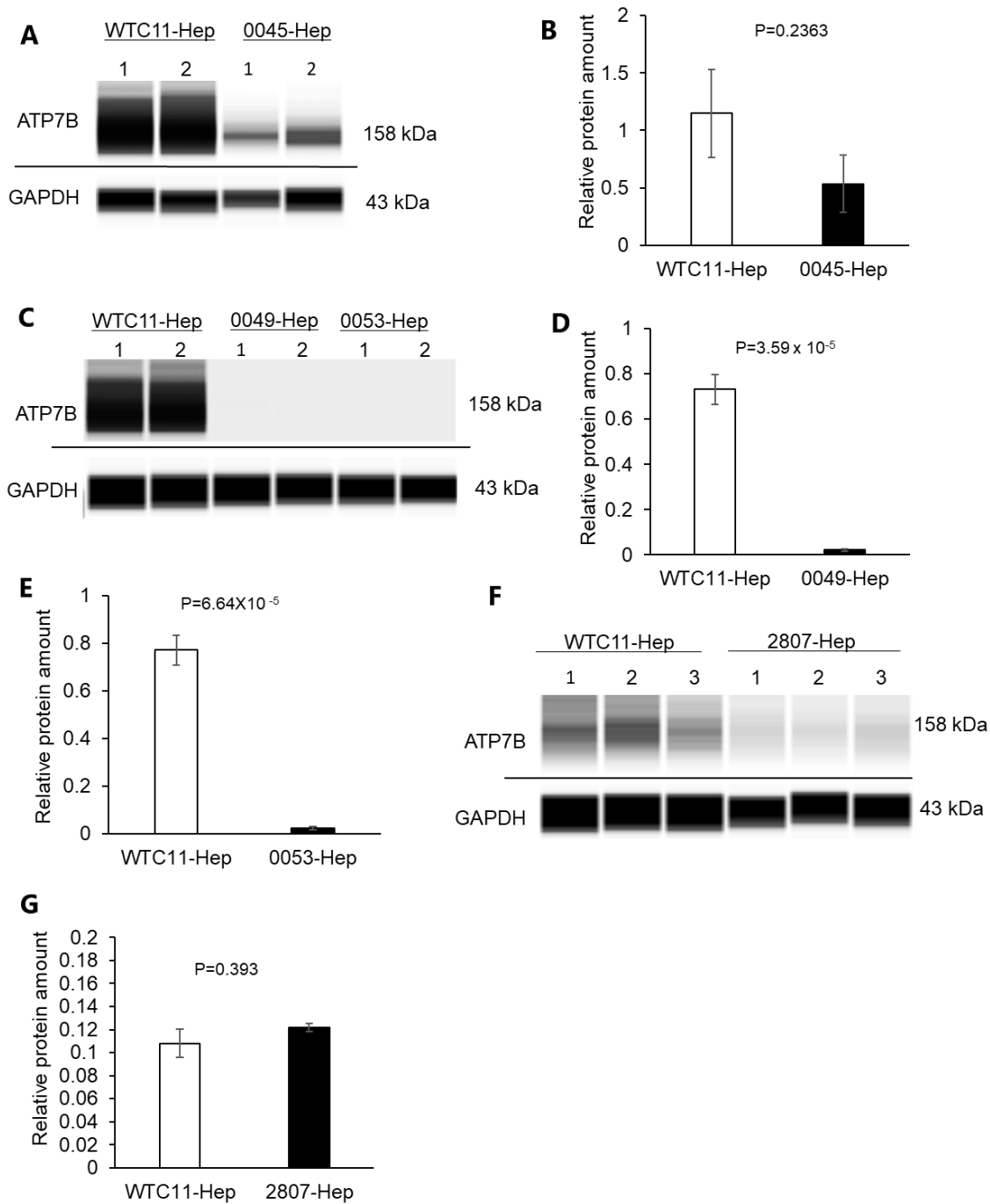


**Figure 11. ATP7B protein detection in four WD iPSCs derived Hepatocyte. A, C and F.** Representative western blot bands of ATP7B in the indicated WD-specific hepatocyte. GAPDH protein was used as a housekeeping control. **B, D, E and G.** Bar graphs showing quantified expression levels of ATP7B protein normalized with the expression levels of

GAPDH protein in the indicated WD iPSC derived hepatocyte. The data obtained from WTC11-Hep were used as the common control for each WD-Hep (0045-Hep, n=4; 0053-Hep, n=6; 0049-Hep, n=7; 2807-Hep, n=3). Data are shown as mean  $\pm$  SEM. P-values were determined by unpaired two-tailed Student's *t*-test.

#### 4.6. Cp expression was consistently decreased in WD iPSCs derived hepatocyte

As a major copper carrier, ceruloplasmin (Cp) attracted my attention for its antioxidative function, iron metabolism as well as an important criterion for WD disease diagnosis. Cp were majorly secreted by the liver. In the hepatocyte, Cp could receive copper ions from ATP7B protein and then been secreted into plasma to deliver these ions throughout the whole body. Next, I examined the Cp expression level of iPSC derived hepatocyte. The RT-qPCR result showed that CP mRNA expression was considerably increased on differentiation day 17 under this differentiation protocol (**Fig. 12**)

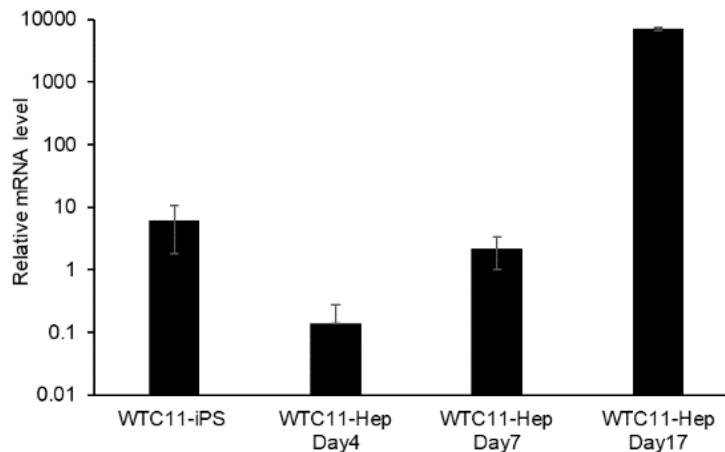


**Figure 12. CP mRNA expression during hepatocyte differentiation in WTC11 iPSCs.** Data are shown as mean  $\pm$ SEM (n=3).

Since WD patients generally secreted low level of Cp, which was supposed to represent the defective ATP7B function. Then I would like to know whether the WD iPSC derived hepatocyte could recapitulate this disease feature *in vitro*. To address this question, CP mRNA expression level and Cp secretion level were determined in WD iPSC derived hepatocytes with RT-qPCR and western blot, respectively. Results showed that Cp mRNA expression level was significantly lower in WD-specific hepatocytes compared with WTC11-derived hepatocytes on differentiation day 17 (**Fig. 13A-D**).

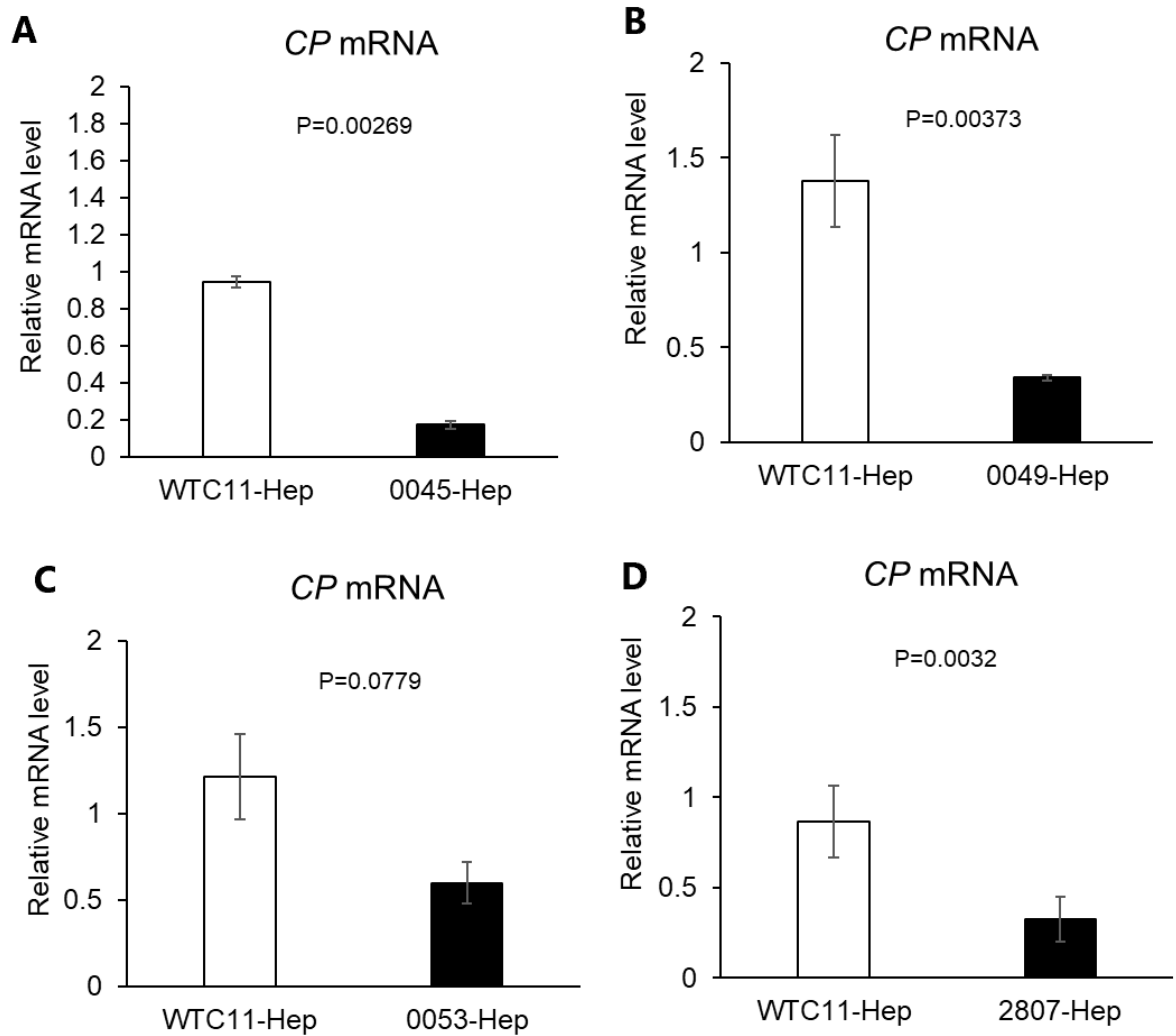


**Figure 13. Cp gene expression in WD-iPSC derived hepatocyte. A-D.** CP mRNA expression in the indicated WD iPSC line derived hepatocyte relative to the WTC11 iPSC derived hepatocyte. Data are shown as mean  $\pm$ SEM (n=3). P-values were determined by unpaired two-tailed Student's *t*-test.

Also, the western blotting results showed that the level of Cp secretion, which was normalized by the amount of secreted ALB to evaluate Cp secretion levels per hepatocyte, was generally lower in WD-specific hepatocytes compared with WTC11-derived hepatocytes (**Fig. 14**). While I especially was interested in

whether the defective ATP7B is the direct reason for the low Cp secretion since it is still lack of evidence for the etiological mechanism of the low Cp in the WD.

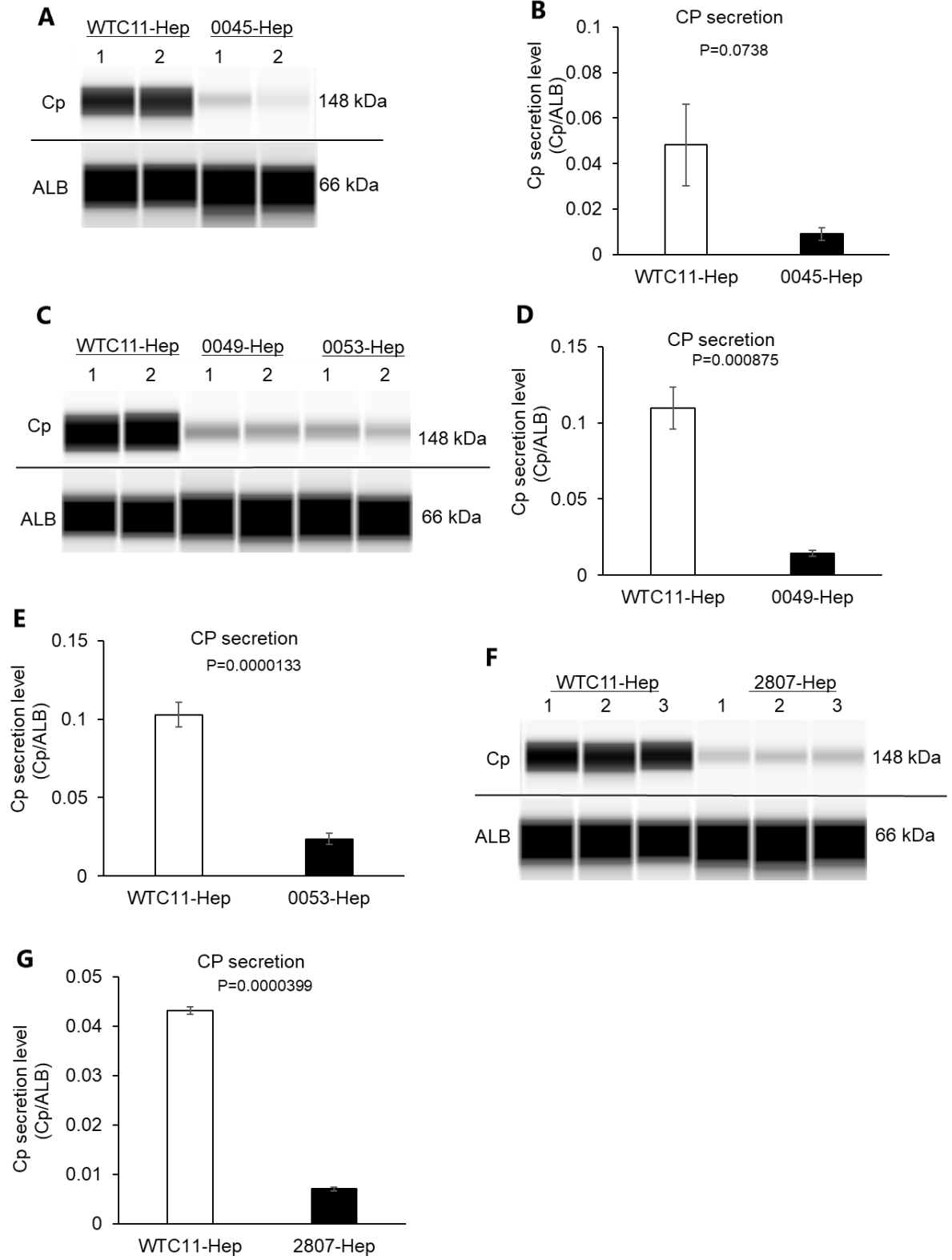


**Figure 14. Cp secretion in WD-iPSC derived hepatocyte. A, C and F.** Representative images of western blot of secreted Cp and ALB proteins by WTC11 derived hepatocyte and the indicated WD-iPSC-derived hepatocyte cultures on differentiation day 17. **B, D, E and G.** Quantified data of Cp protein secretion levels of indicated WD specific hepatocyte after normalized with ALB. WTC11 derived hepatocyte was used as the common control for each WD specific hepatocyte (0045-Hep, n=7; 0053-Hep, n=7; WD0049-Hep, n=6; 2807-Hep, n=3). Data are shown as mean  $\pm$  SEM. P-values were determined by unpaired two-tailed Student's *t*-test.

#### **4.7. ATP7B expression and Cp secretion in *ATP7B* deficient iPSC derived hepatocyte**

To verify the effect of ATP7B on the ceruloplasmin secretion, I performed the loss-of-function of ATP7B with isogenic backgrounds in iPSC-derived hepatocyte models. I adopted a *ATP7B*-deficient iPSC line, which is generated by Dr. Miyaoka and Dr. Takahashi. This iPSC cell line was generated from WTC11 iPSC line using CRISPR-Cas9 system by them [40]. In the ATP7B deficient iPSC line, 7 bp was deleted in *ATP7B* exon 1 in one allele, and 104 bp spanning exon 1 and intron 1 was deleted in the other allele according to their sequence data. The deletion region on two alleles includes the translation starting codon. It indicated the ATP7B mRNA cannot transcript as usual in this *ATP7B*-deficient iPSC line. Hereafter, ATP7B-deficient iPSC line was named as ATP7BKO iPSCs. ATP7BKO iPSCs was differentiated into hepatocyte with the above-mentioned differentiation protocol. Hepatic differentiation capability of the ATP7BKO iPSCs was evaluated with hepatic related markers expression. The results showed that

there is a high percentage cells being positive to SOX17 and GATA6, as the endoderm markers on differentiation day 5 (**Fig. 15A and B**). ATP7BKO iPSCs expressed the similar level of A1AT and AFP mRNA as their original iPSC line on differentiation day 17 (**Fig. 15C and D**). On the same differentiation day, hepatic protein (HNF4A/AFP/ALB) expression were also examined, and the results showed that ATP7BKO iPSCs derived hepatocyte were highly expressing these proteins (**Fig. 15E-G**). Collectively, these results indicated that ATP7BKO iPSCs possessed the similar hepatic differentiation capability as its parental line.

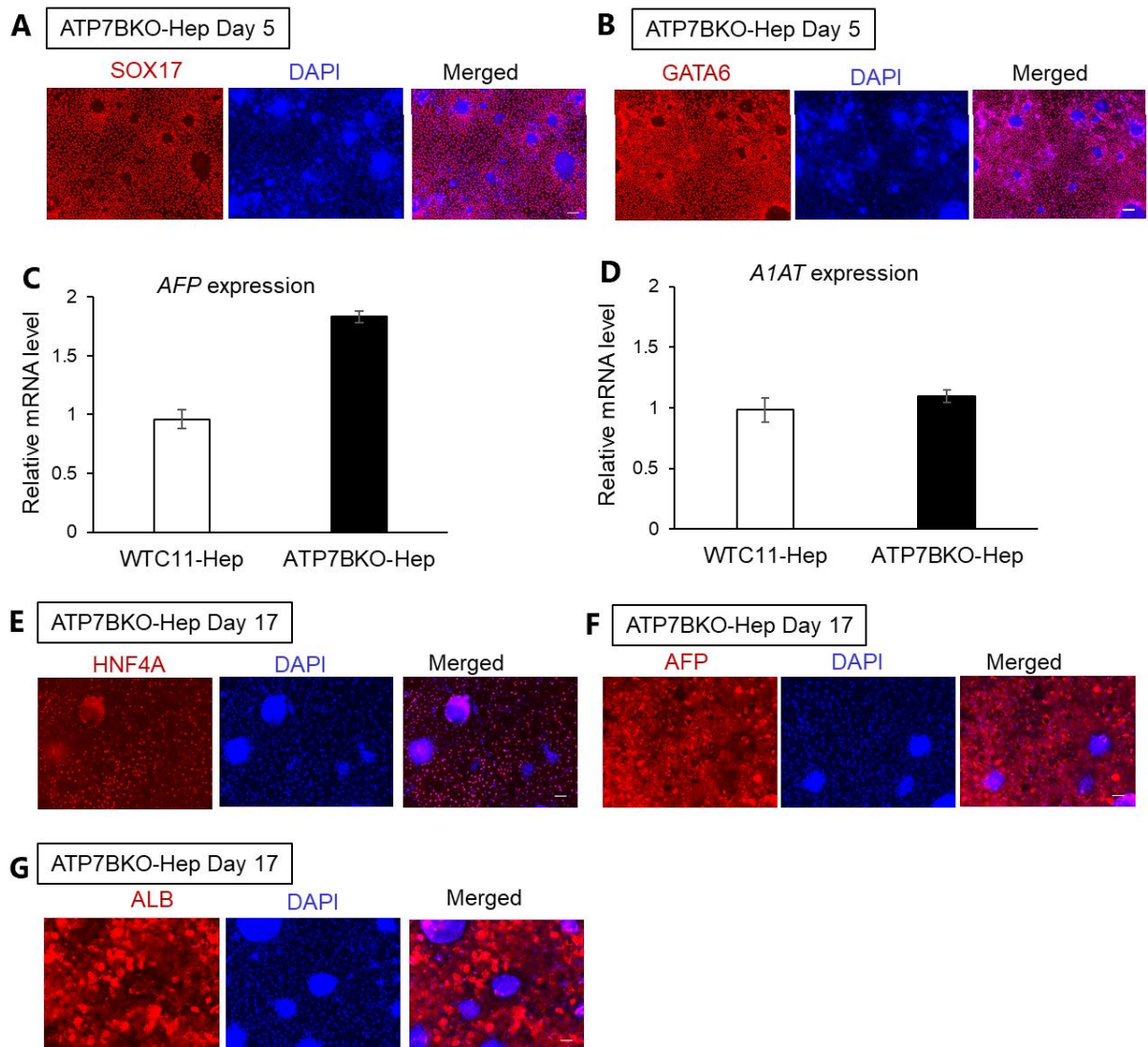


**Figure 15. Hepatocyte differentiation of ATP7BKO iPSCs.** **A** and **B**. Representative immunostaining images showing the expression of endoderm markers, SOX17 (**A**) and GATA6 (**B**), on differentiation day 5 of ATP7BKO iPSCs. Scale bar is 100  $\mu$ m. **C** and **D**. The gene expression of hepatic markers, *AFP* (**C**) and *A1AT* (**D**), detected by RT-qPCR in hepatocytes derived from parental WTC11 and ATP7BKO iPSC lines. Bar graphs show the mean  $\pm$  SEM ( $n=3$ ). **E-G**. Representative immunostaining images showing the expression of hepatocyte markers, HNF4A (**E**), AFP (**F**), and ALB (**G**), on differentiation day 17 of ATP7BKO iPSCs. Scale bar is 100  $\mu$ m.

Also, ATP7B gene and protein expression was examined in these ATP7BKO iPSCs derived hepatocytes with RT-qPCR and western blotting, respectively. ATP7BKO iPSCs derived hepatocytes showed comparable ATP7B gene and protein expression levels as WTC11-derived hepatocytes (**Fig. 16A-C**). These results indicated that gene editing in *ATP7B* did not interfere ATP7B expression in both transcriptional and post-transcriptional levels, possibly due to the generation of alternative start codons after its gene edition. Nonetheless, mRNA expression level and secretion level of Cp were significantly decreased in ATP7BKO iPSCs derived hepatocytes (**Fig. 16D-F**). These results indicated that the functionality of the ATP7B protein expressed in these ATP7BKO iPSCs derived hepatocytes was severely compromised. Collectively, our results demonstrated that the defective ATP7B gene could cause Cp expression level in iPSC-derived hepatocytes.

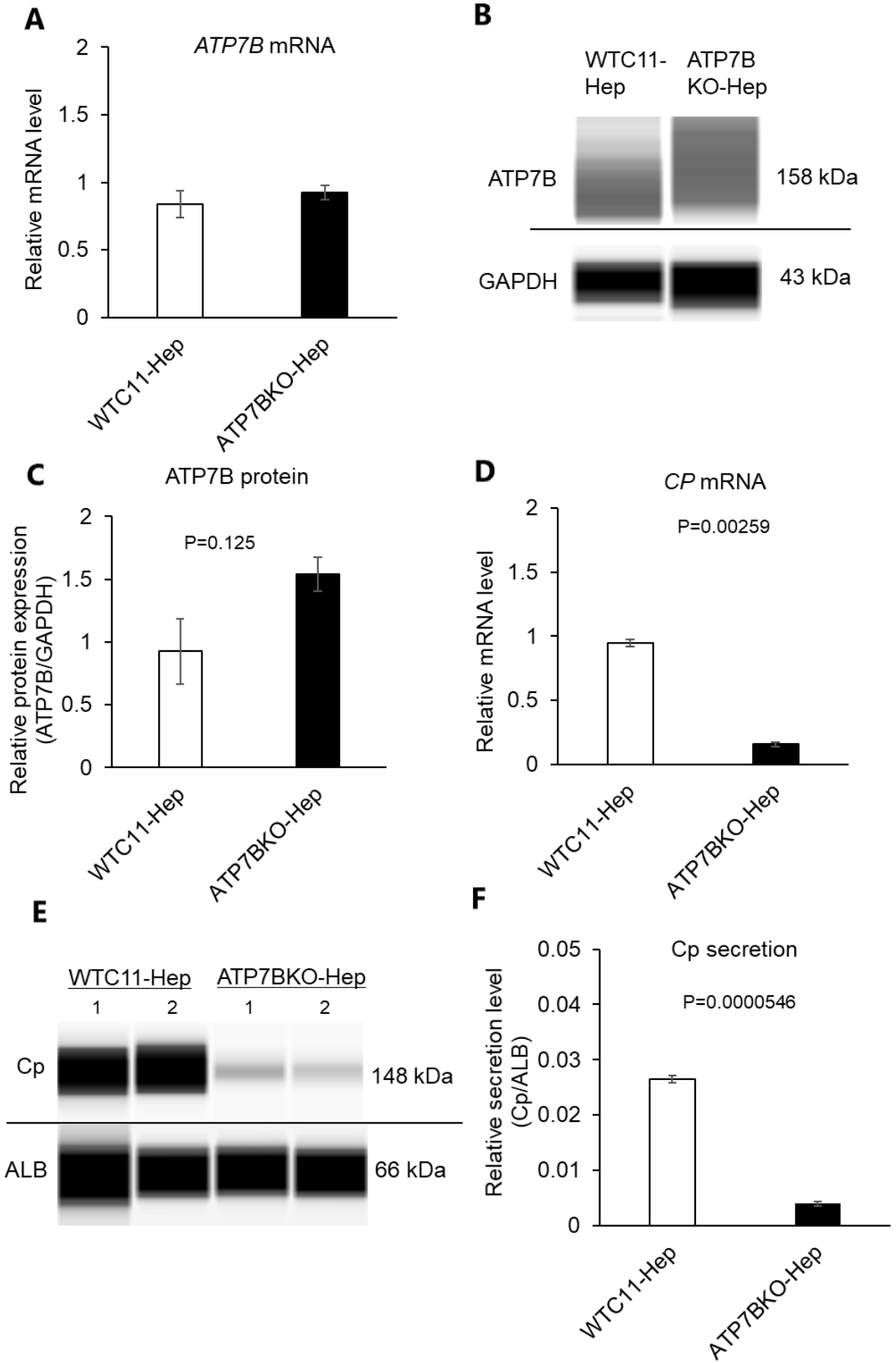


**Figure 16. ATP7B and Cp expression in the ATP7BKO-Hep. A.** The expression level of *ATP7B* mRNA in WTC11-Hep and ATP7BKO-Hep. Data are shown as mean  $\pm$  SEM (n=3). **B.** Representative image of western blot data of ATP7B and GAPDH proteins from parental WTC11- and ATP7BKO-iPSC-derived hepatocyte cultures on differentiation day 17. **C.** Quantified data of ATP7B protein expression levels after normalized with GAPDH protein. Data are shown as mean  $\pm$  SEM (n=3). **D.** The expression level of *CP* mRNA in WTC11-Hep and ATP7BKO-Hep. Data are shown as mean  $\pm$  SEM (n=3). P-values were determined by unpaired two-tailed Student's *t*-test. **E.** Representative image of western blot bands of secreted Cp and ALB proteins by WTC11- and ATP7BKO-Hep on differentiation day 17. **F.** Quantified data of secreted CP protein levels after normalized with ALB protein in WTC11-Hep and ATP7BKO-Hep. Data are shown as mean  $\pm$  SEM (n=3). P-values were determined by unpaired two-tailed Student's *t*-test.

#### **4.8. ATP7B expression and Cp secretion in R778L homozygous and R778L heterozygous iPSC derived hepatocyte**

Conversely, I asked whether restoring the ATP7B function could rescue the Cp secretion. To address this question, I further adopted the other two iPSC lines, R778L homozygous and R778L heterozygous mutation carrying WD iPSC lines, which were provided by Dr. Miyaoka and Dr. Takahashi. R778L heterozygous iPSC line was the result of CRISPR-Cas9-based gene correction on one WD-iPSC line carrying predominated homozygous mutation (R778L), which was generated previously[24]. Then these two iPSC lines were differentiated into hepatocyte with above protocol. Hepatic differentiation capability of the corrected R778L-heterozygous iPSC subclone and the original R778L-homozygous iPSC line was examined by immunostaining and RT-qPCR. These two iPSC lines

expressed comparable levels of endoderm markers (SOX17/GATA6) on differentiation day 5 (**Fig. 17A and B**). They could also express significantly high levels of hepatic markers (HNF4A/AFP/ALB) on differentiation day 13 (**Fig. 17C and D**). Hepatic genes expression was examined on differentiation day 17, and RT-qPCR results showed these two iPSC lines expressed similar level of these two genes (**Fig. 17E and F**). All of our results indicated that these two iPSC lines possessed the similar hepatic differentiation potential.

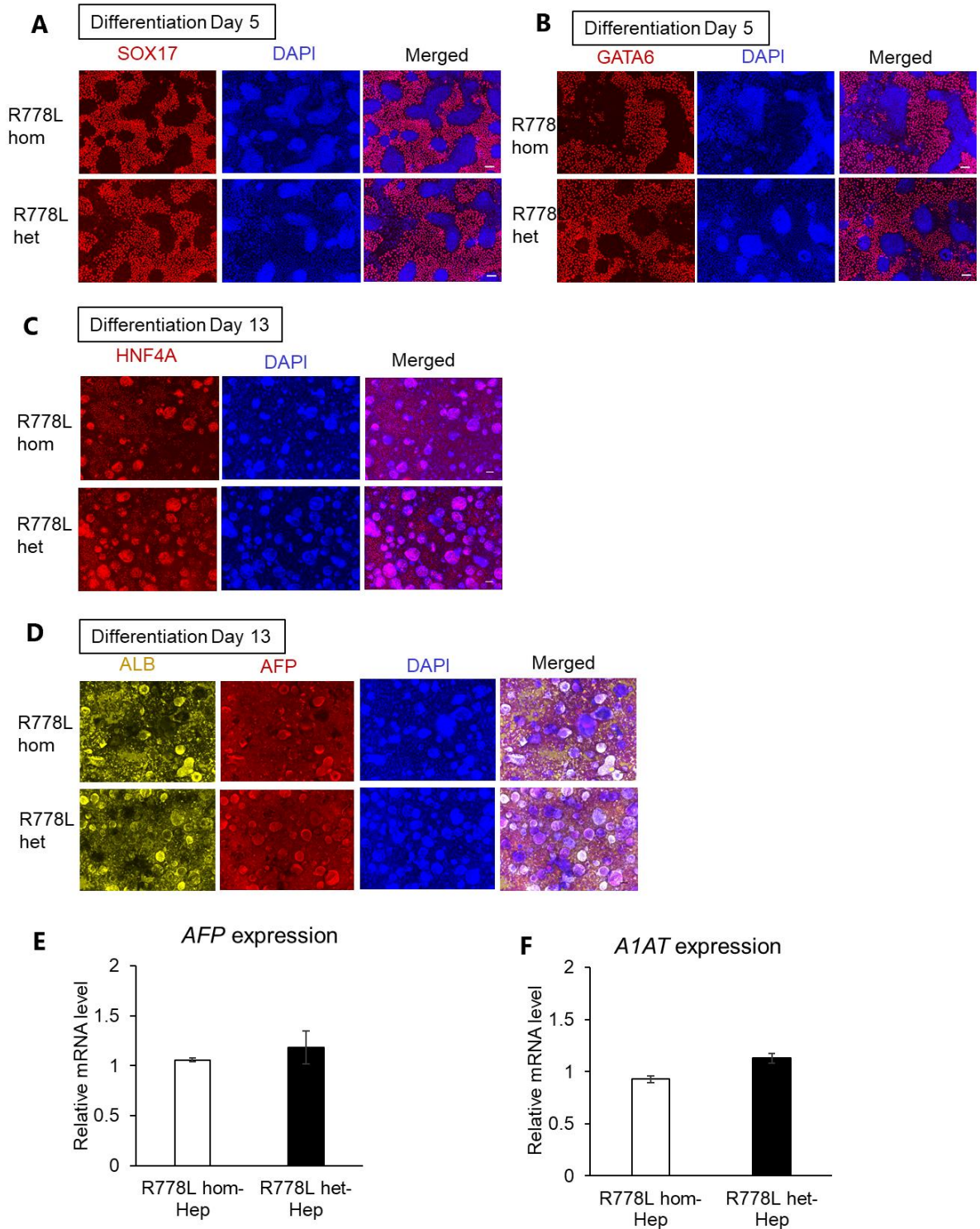


**Figure 17. Similar hepatocyte differentiation capacity of *ATP7B* R778L-heterozygous iPSCs and R778L-homozygous iPSCs. A and B.** Representative immunostaining images showing the expression of endoderm markers, SOX17 (A) and GATA6 (B), on differentiation day 5 of *ATP7B*

R778L- heterozygous and -homozygous iPSC lines. Scale bar is 100  $\mu$ m. **C** and **D**.

Representative immunostaining images showing the expression of hepatocyte markers, HNF4A

**(C)**, AFP and ALB **(D)**, on differentiation day 13 of *ATP7B* R778L-heterozygous and -

homozygous iPSC lines. Scale bar are 100  $\mu$ m. **E** and **F**. The gene expression of hepatic markers,

*AFP* **(E)** and *A1AT* **(F)** detected by RT-qPCR in day 17 hepatocytes derived from *ATP7B* R778L-

heterozygous and -homozygous iPSC lines (n=3). Bar graphs show the mean  $\pm$  SEM.

To examine the effect of gene correction of *ATP7B* on the *ATP7B* protein and function, *ATP7B* mRNA and protein levels were examined in these iPSC-derived hepatocytes. Both of two iPSC lines expressed similar levels of *ATP7B* mRNA **(Fig. 18A)**, while the R778L-heterozygous line expressed a significantly higher level of *ATP7B* protein **(Fig. 18B and C)**. Cp mRNA and secretion levels were further examined in these conditions. This R778L-heterozygous subclone expressed significantly higher levels of mRNA **(Fig. 18D)** and secreted higher level of Cp protein than those of the original R778L-homozygous line **(Fig. 18E and F)**. These results suggested that heterozygous correction of R778L rescued Cp expression and secretion levels as well as *ATP7B* protein expression and function. Collectively, these results demonstrated that the gain-of-function of *ATP7B* could be manifested by the R778L mutation site correction iPSC line derived hepatocyte.

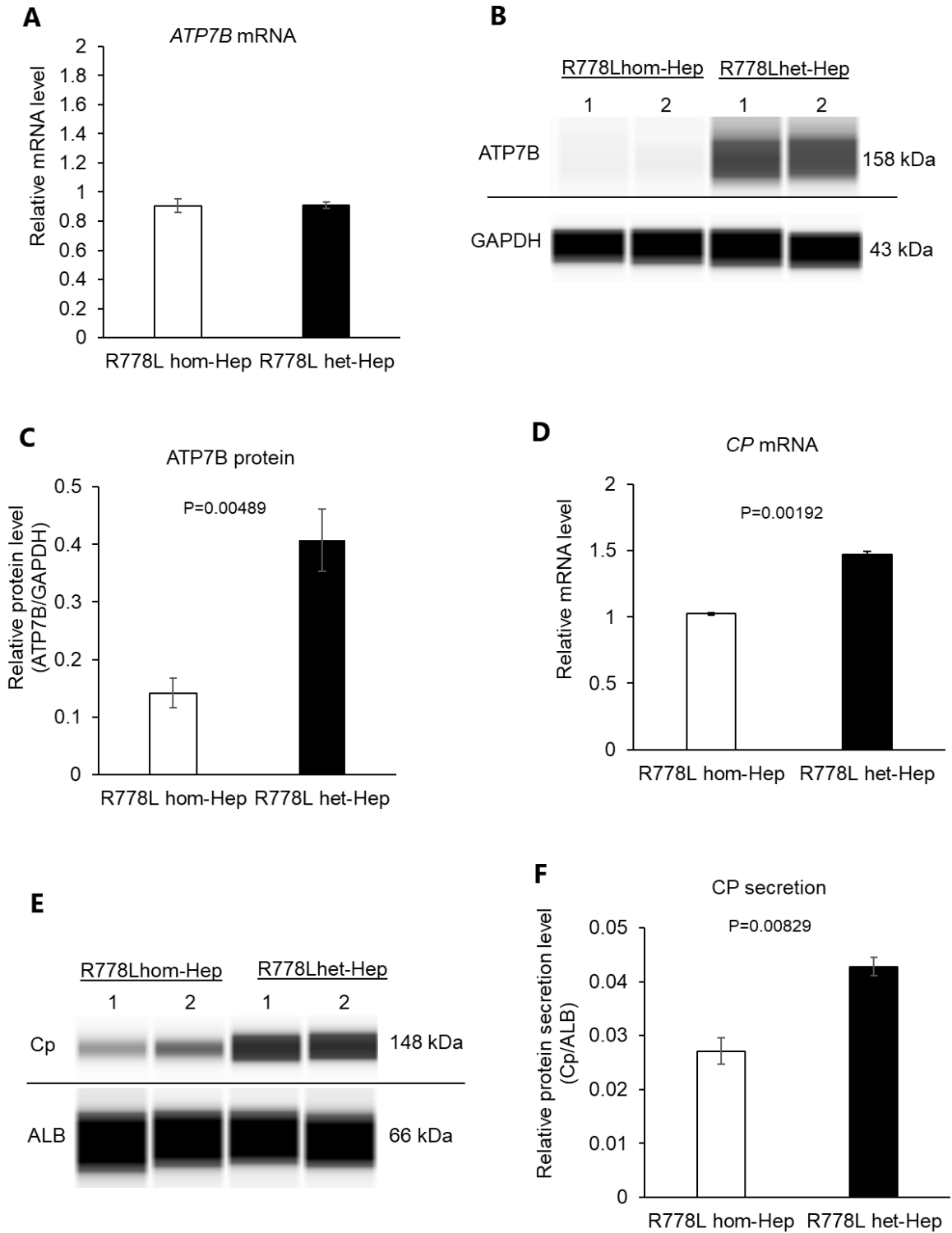


**Figure 18. *ATP7B* expression and Cp secretion in *ATP7B* R778L homozygous iPSCs and R778L heterozygous iPSCs derived hepatocyte.** **A.** The expression level of *ATP7B* mRNA in R778L hom- and R778L het-iPSC-derived hepatocytes on differentiation day 17. Data are shown

as mean  $\pm$  SEM (n=3). **B.** Representative image of western blot data of ATP7B and GAPDH proteins from parental R778Lhom- and R778Lhet-iPSC-derived hepatocytes on differentiation day 17. **C.** Quantified data of ATP7B protein expression levels after normalized with GAPDH protein. Data are shown as mean  $\pm$  SEM (n=3). **D.** Expression levels of *CP* mRNA in R778Lhom-Hep and R778Lhet-Hep detected by RT-qPCR. Data are shown as mean  $\pm$  SEM (n=3). P-values were determined by unpaired two-tailed Student's *t*-test. **E.** Representative image of western blot bands of secreted Cp and ALB proteins by R778Lhom-Hep and R778Lhet-Hep on differentiation day 17. **F.** Quantified data of secreted CP protein levels after normalized with ALB protein in R778L hom-Hep and R778L het-Hep. Data are shown as mean  $\pm$  SEM (n=3). P-values were determined by unpaired two-tailed Student's *t*-test.

#### **4.9. Cp secretion-based drug screening to explore new therapeutic target of WD**

From the above results, the decreased level of secreted Cp is a robust and convenient indicator of ATP7B dysfunction in WD-specific iPSC-derived hepatocytes. Assuming up-regulating Cp secretion capability of these WD-specific hepatocytes might be helpful to relieve excessive copper-induced symptoms. Then a chemical screening system were developed to evaluate Cp secretion levels in iPSC-derived hepatocytes using an automatic capillary western blot device (**Fig. 19A**). In this study, eleven candidate chemicals, which had been reported to affect ATP7B activity, were screened in these five WD-specific iPSC-derived hepatocytes. Among these 11 candidate chemicals, only ATRA significantly increased Cp secretion levels of HPS0045 iPSC derived

hepatocytes in the comparison with DMSO treated control conditions (**Fig. 19B and C**).

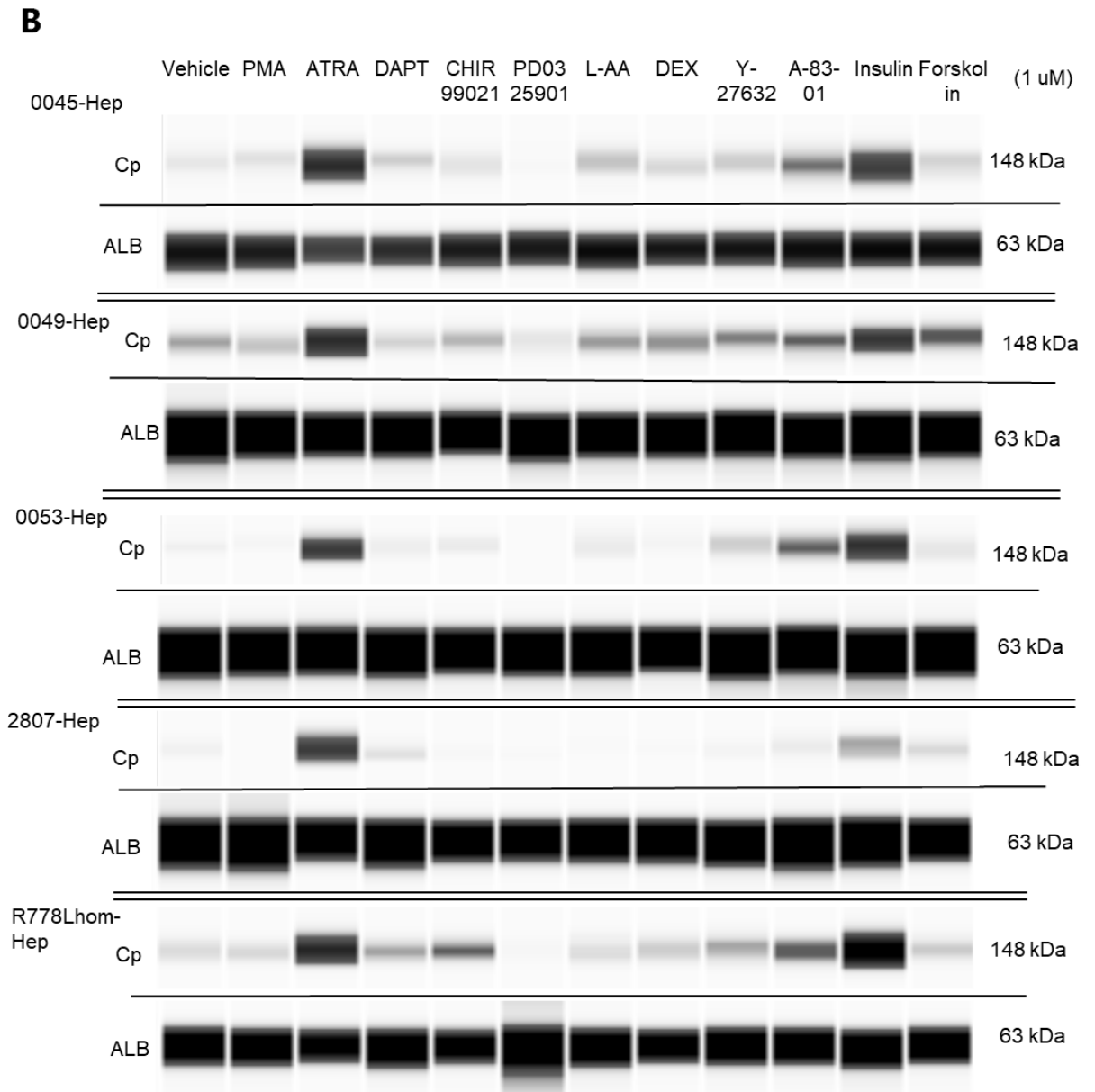
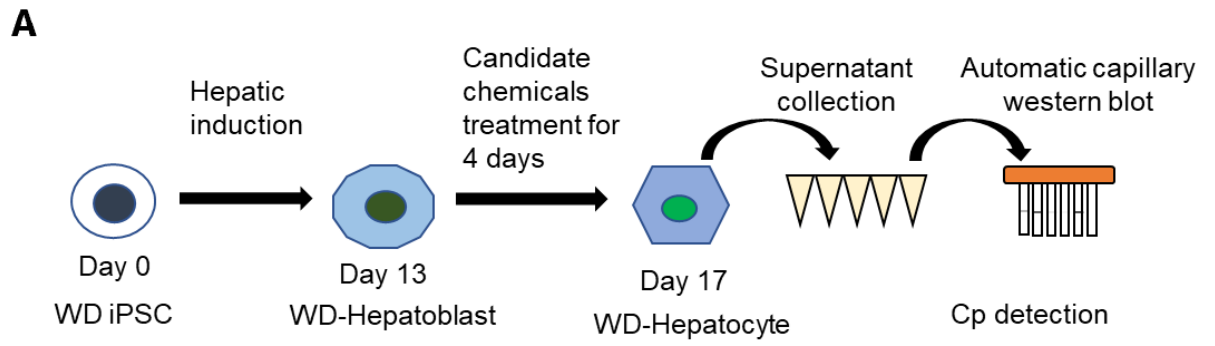


**Figure 19. Cp secretion-based drug screening in five WD-iPSC derived hepatocytes. A.**

Schema of Cp secretion-based drug screening. **B.** Representative image of western blot data of secreted Cp and ALB proteins by indicated WD iPSC derived hepatocyte on differentiation day 17 after treated with indicated drugs for 4 days.

The quantitative result of Cp-based chemical screening from 5 WD iPSC lines derived hepatocyte was shown as in **Fig. 20.**

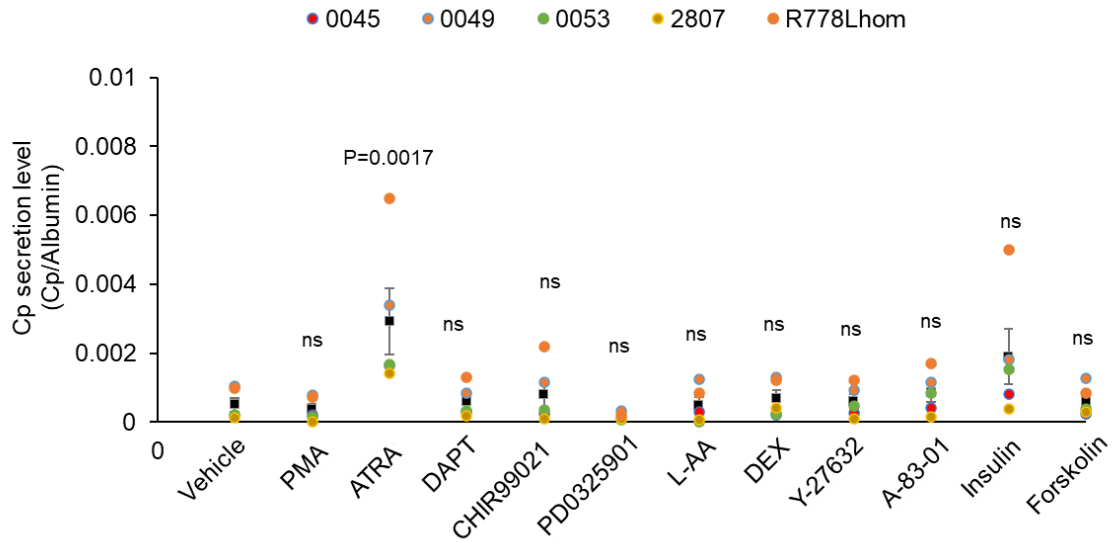


**Figure 20. ATRA increase CP secretion in WD-iPSC-derived hepatocytes.** Quantified data of

Cp secretion level after normalized with ALB, dot colors indicate data from different WD-Hep.

Data are shown as mean of Cp secretion level from five WD-Hepatocyte  $\pm$  SEM. Statistical

significance was determined by Dunnett's test relative to DMSO-treated conditions (vehicle).

Furthermore, the effect of ATRA on *CP* mRNA expression was examined with RT-qPCR. The result showed that ATRA treatment could significantly upregulate *CP* gene expression without having obvious effects on the expression of other hepatic genes in these 5 WD-specific hepatocytes (**Fig. 21**). These results suggested that ATRA rescued decreased expression and secretion of Cp in WD-specific hepatocytes without obviously affecting hepatocyte identity.

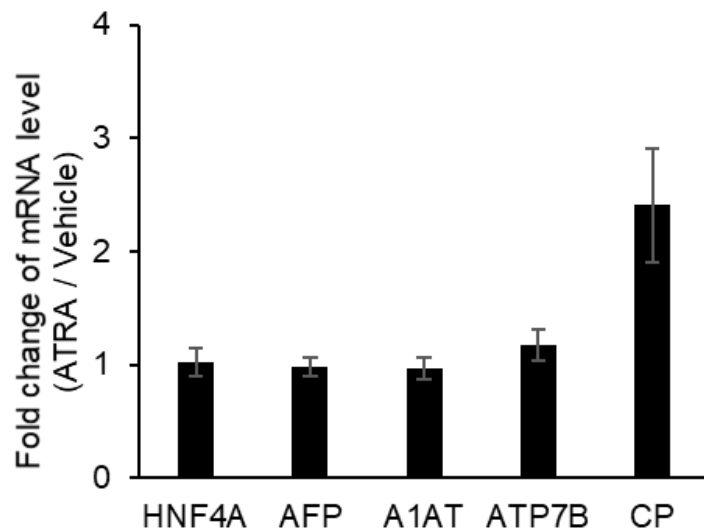


**Figure 21.** Expression levels of *HNF4A*, *AFP*, *A1AT*, *ATP7B* and *CP* mRNA in 5 WD specific hepatocyte on differentiation day 17 after treated with DMSO (vehicle) or ATRA for 4 days quantified by RT-qPCR. Bar graph show mean  $\pm$  SEM (n=3).

As we know, ATRA belongs to retinoid family molecules and regulates a wide variety of physiological functions through its nuclear receptors, known as the classical retinoic acid receptors (RARs) and nonclassical retinoid X receptors (RXRs) [41, 42]. To further verify and extend the effect of ATRA on secret levels of Cp in WD-Hep clinically-used retinoids, 4 clinically-approved retinoid

derivatives were employed; Tazarotene and Am80 are RAR-selective retinoids [43, 44], and Bexarotene and cis-4,7,10,13,16,19-Docosahexaenoic acid (DHA) are RXR-selective retinoids [45, 46]. Effects of these four retinoids and ATRA on Cp secretion were further examined in WD-specific hepatocytes. These retinoids except for DHA increased Cp secretion in hepatocytes derived from iPSC lines of HPS0045 (**Fig. 22A and B**), HPS0053 (**Fig. 22C and D**), and R778L-homozygous mutant (**Fig. 22E and F**). These results suggested that retinoid derivatives rescued decreased Cp expression and secretion in WD-specific hepatocytes.

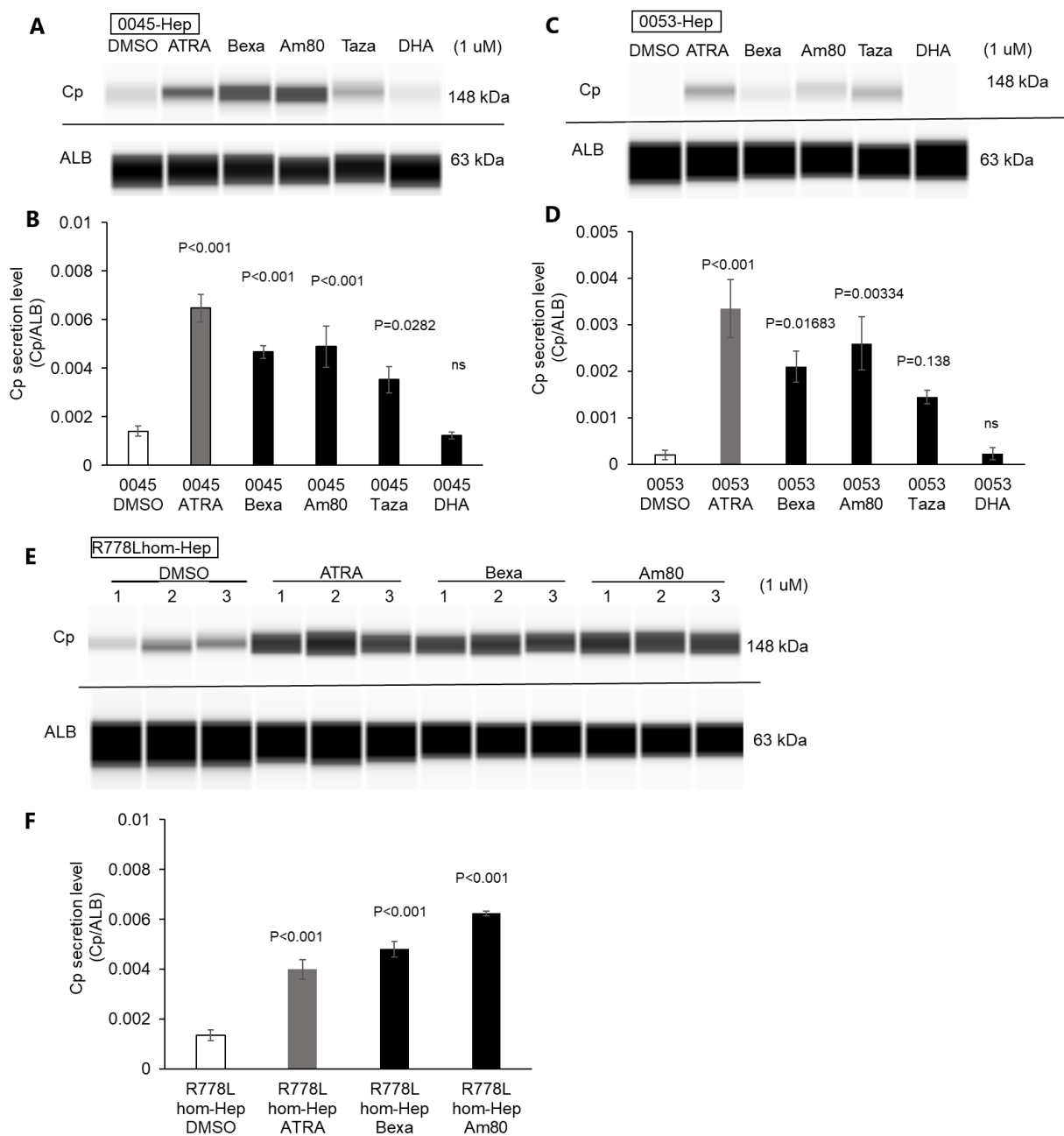


**Figure 22. Effect of RAR and RXA agonists on the Cp secretion.** **A** and **C**. Representative images of western blots showing Cp secretion level of 0045-Hep (**A**) and 0053-Hep (**C**) on day 17 after being treated with indicated two RXRs and two RARs agonists for 4 days. **B** and **D**. Quantified data of secreted CP protein levels after normalized with secreted ALB protein in 0045-Hep (**B**) and 0053-Hep (**D**) treated with indicated two RXRs and two RARs agonists. Data are

shown as mean  $\pm$  SEM (n=4). P-values were determined by Dunnett's test relative to DMSO-treated condition (vehicle). **E.** Images of western blots showing Cp secretion level of R778L hom-Hep with three replicates. **F.** Quantified data of secreted Cp protein levels after normalized with secreted ALB protein level in R778L hom-Hep after treated with indicated RXR and RAR agonists. Data are shown as mean  $\pm$  SEM (n=3).

#### **4.10. Transcriptome comparison between WD-Hep and WT-Hep**

RNA-seq analysis was performed to identify the global gene expression patterns differences between WD-specific hepatocytes and WT iPSC derived hepatocyte. Six WD-specific hepatocytes and 6 healthy-donor (HD) hepatocytes were compared in total (**Fig. 23A**). From this comparison, 238 genes were significantly down-regulated (FDR < 0.05), and 431 genes were significantly up-regulated (FDR < 0.05) in WD-Hep (**Fig. 23B**). Of note, *CP* was included in the genes that were significantly down-regulated. Next, enrichment analysis of biological pathways and gene ontology on these differentially-regulated genes were performed for the downstream analysis. In the HMDB (Human Metabolite DataBase) program, RA was identified as the top metabolite which was related with these down-regulated genes in WD-Hep (**Fig. 23C**). It indicated the RA related metabolic pathway was down-regulated in the WD iPSC derived hepatocyte group. In NCATS (National Center for Advancing Translational Sciences) BioPlanet program, lipid and lipoprotein metabolisms were enriched by the up-regulated genes in WD-Hep (**Fig. 23D**). In the DisGeNET program, liver neoplasms, fatty liver, and steatohepatitis were the top associated diseases

enriched by the up-regulated genes in WD-Hep (**Fig. 23E**). These results suggested that the lipid metabolic related pathway was dysregulated in the WD iPSC derived hepatocyte group.

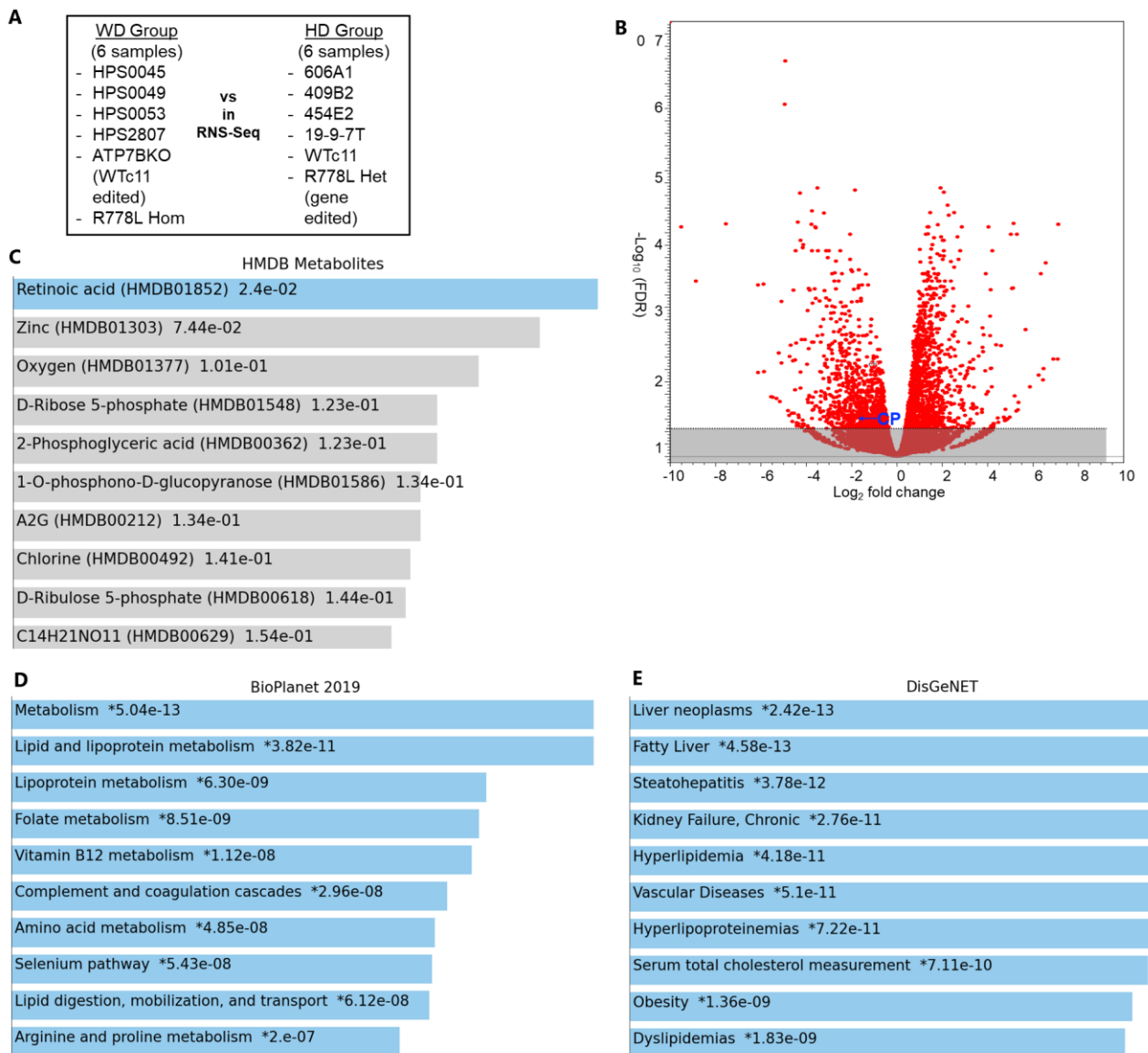


**Figure 23. Global transcriptome analysis in WD-iPSC and WT-iPSC-derived hepatocytes. A.** Schema of RNA-seq sample arrangement. **B.** Volcano plot shows Log<sub>2</sub> fold change as X-axis and -log<sub>10</sub> (FDR) as Y-axis. All the genes were plotted in red circle. CP gene was indicated by a

blue arrow. Non-significant genes with  $FDR \geq 0.05$  was masked in gray. **C.** A bar chart showing candidate metabolites using HMDB (human metabolome data base) Metabolites program from down-regulated genes. Metabolite names (HMDB metabolite ID) and values of  $-\log_{10}(P\text{-value})$  are shown. **D.** A bar chart showing candidate pathways using NCATS (National Center for Advancing Translational Sciences) BioPlanet program from up-regulated genes. Pathway names and values of  $-\log_{10}(P\text{-value})$  are shown. **E.** A bar chart showing candidate disease types using DisGeNET program from up-regulated genes. Disease names and values of  $-\log_{10}(P\text{-value})$  are shown.

#### **4.11. ATRA suppresses oleic acid-induced reactive oxygen species (ROS) production in WD-specific hepatocytes**

Our transcriptome analysis on WD-specific hepatocytes above indicated that abnormal gene expression was related to liver dysfunctions and lipid metabolism. Hepatic steatosis is one of the disease features presented by a large part of WD patients, which may be caused by abnormal lipid metabolism in response to copper accumulation in WD patients [19, 47, 48]. Although molecular mechanisms between copper accumulation and abnormal lipid metabolism in WD remain elusive, ROS (reactive oxygen species) plays a common role in these two biological processes [19, 48, 49]. Thus, to recapitulate the hepatic steatosis disease features, steatosis modeling was performed in WD-Hep by oleic acid treatment. The steatosis modeling assay system was illustrated as in **Fig. 24A**. Then, lipid accumulation and ROS production were evaluated in WD-specific hepatocytes exposed to different concentrations of oleic acid by fluorescent imaging with specific chemical probes. Lipid droplets were becoming

enlarged and outstanding in the WD-derived hepatocytes with the concentrations of oleic acid increase. ROS production was also increased along with the increasing concentrations of oleic acid treatment in WD-specific hepatocytes (**Fig. 24B-E**). These results suggested that the lipid accumulation could cause ROS production increase.

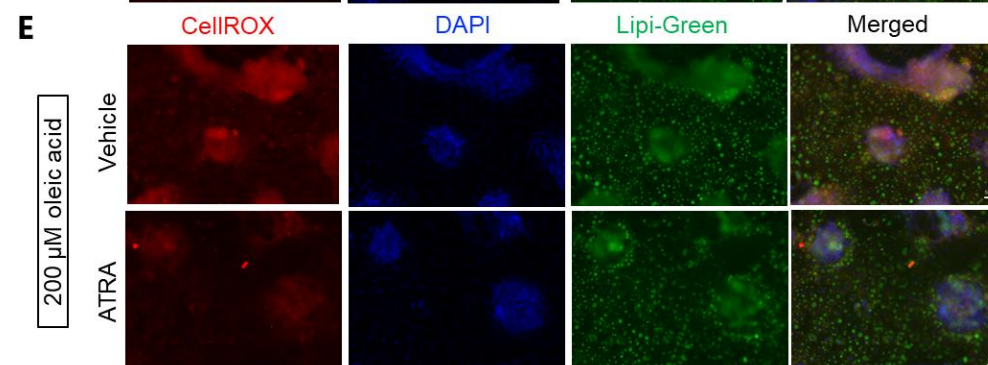
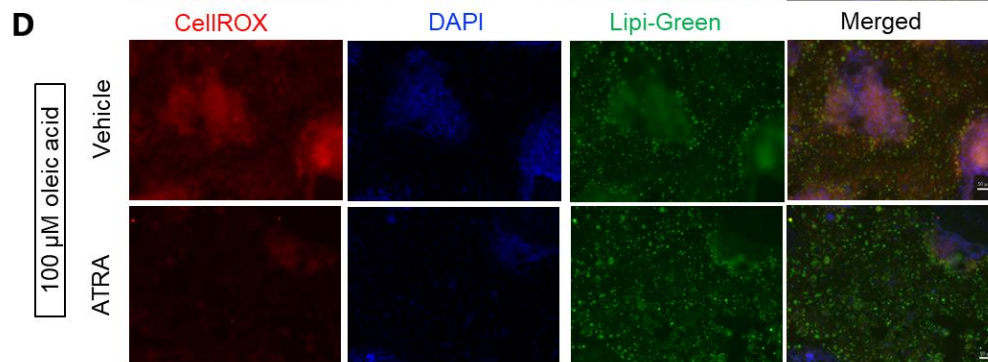
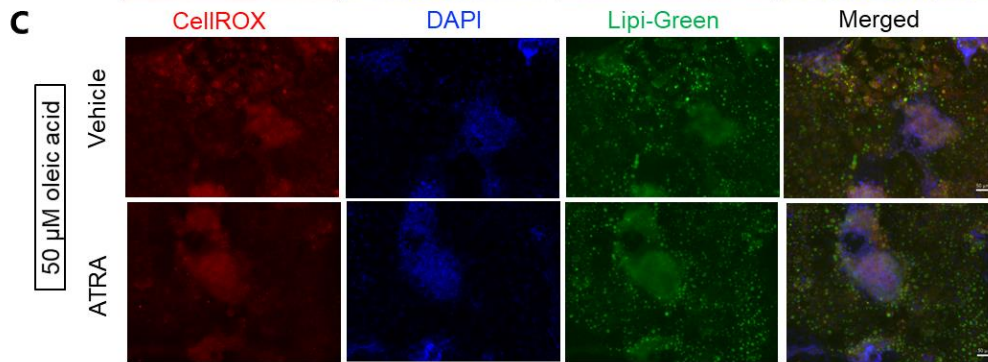
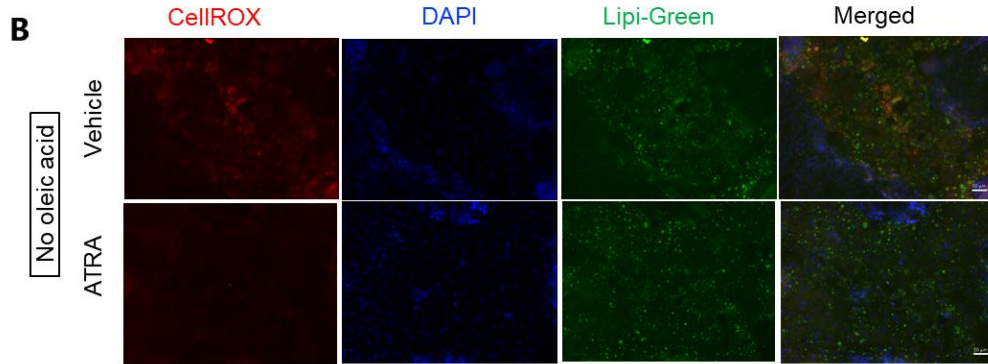
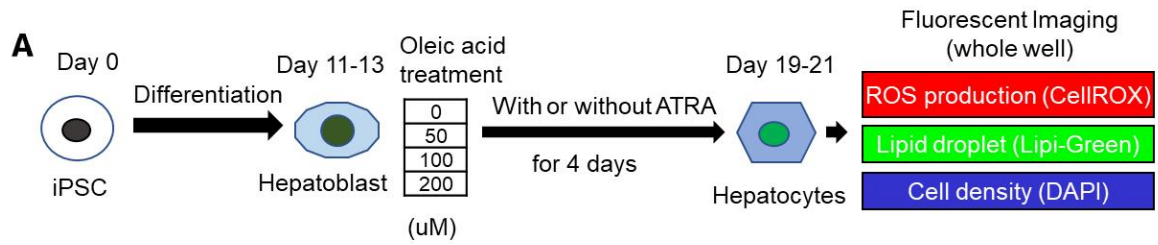


**Figure 24. ATRA decreases oleic acid-induced ROS production in WD-iPSC-derived**

**hepatocytes. A.** Schema of a cellular assay of ROS production and lipid accumulation in WD-iPSC-derived hepatocytes treated with different concentrations of oleic acid with or without ATRA. **(B-E)** Magnified lipid fluorescent images of CellROX, DAPI and Lipi-Green in HPS0045-derived hepatocytes on differentiation day19 after oleic acid treatment at the indicated concentration for 8 days with or without ATRA for 4 days. Scale bars are 50  $\mu\text{m}$ .

To evaluate the ROS production and lipid accumulation, the fluorescent intensity was calculated from these tiled whole-well images (**Fig. 25A-D**). The quantitative result of ROS fluorescent intensity from 4 WD-specific hepatocyte showed that the treatment of ATRA could reduce ROS production in the oleic acid-treated WD-derived hepatocytes (**Fig. 26**)

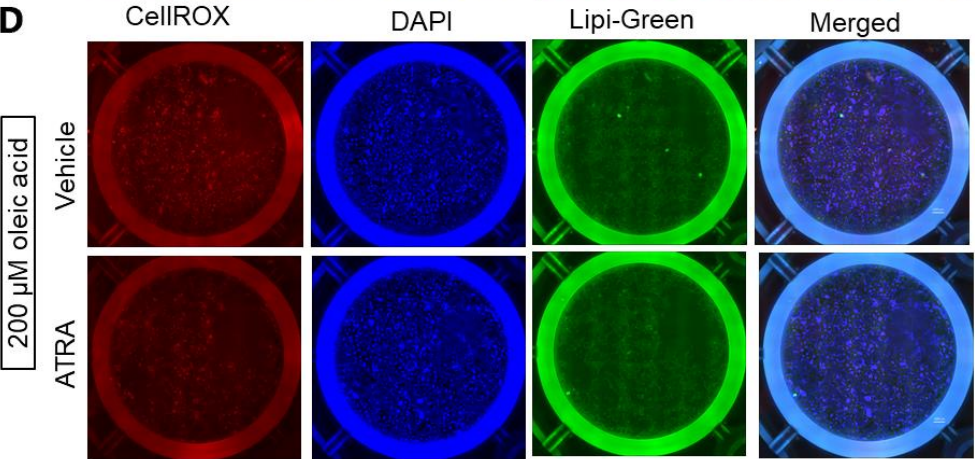
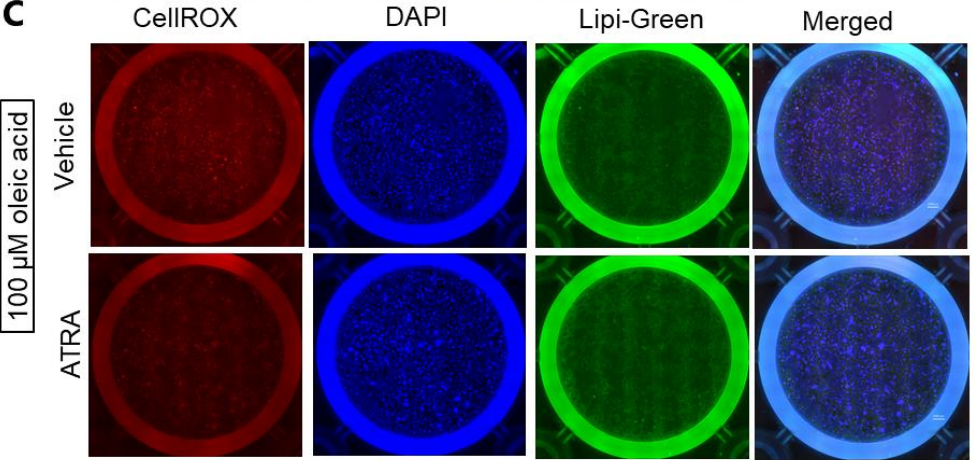
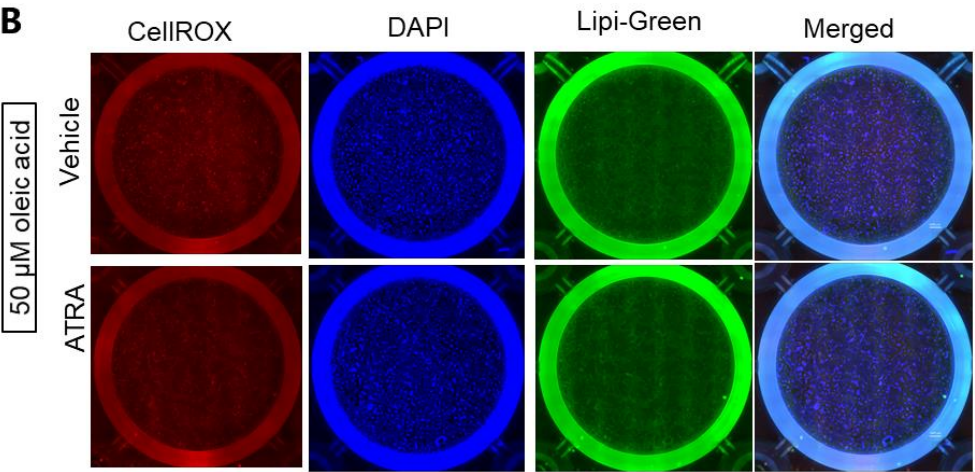
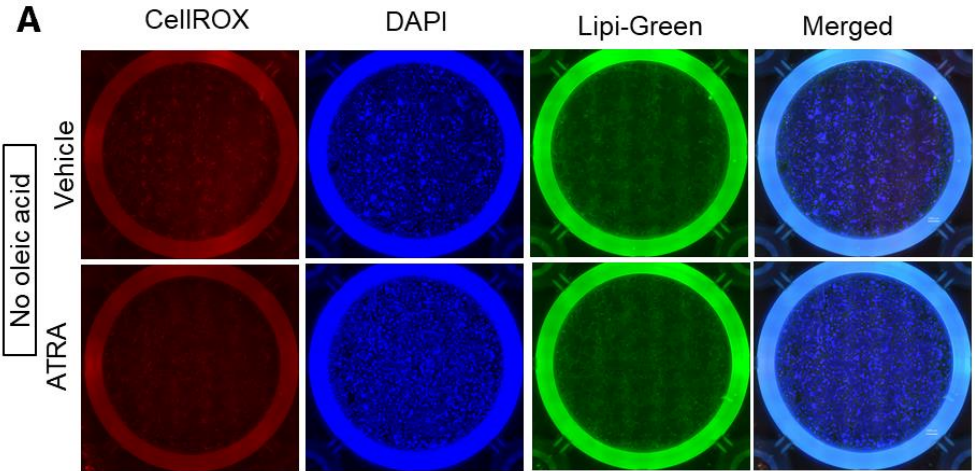


**Figure 25. Tiled whole-well fluorescent images to evaluate ROS production and lipid accumulation in WD-hepatocyte. A-D.** Tiled whole-well fluorescent images of CellROX Deep Red, DAPI, and Lipi-Green in HPS0045-derived hepatocytes after oleic acid treatment at the indicated concentrations for 8 days with or without ATRA for 4 days. Scale bar is 1000  $\mu$ m.

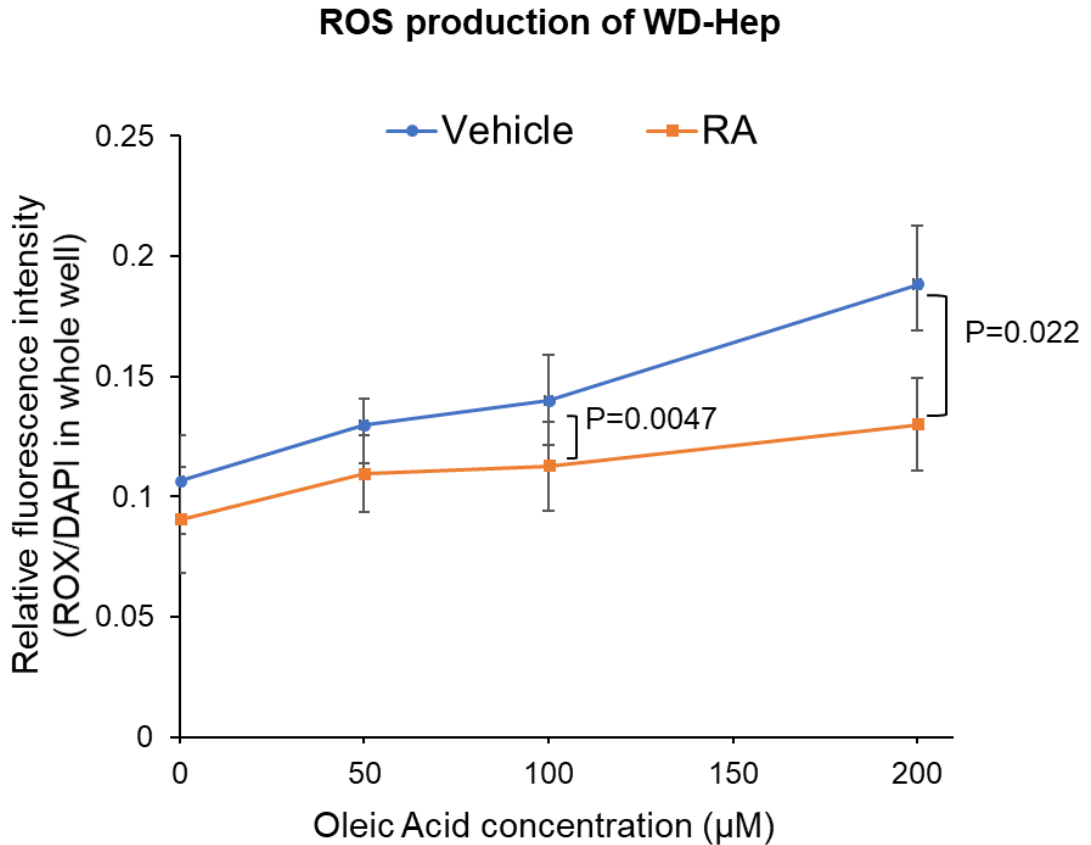


**Figure 26. Quantified ROS production in four WD iPSC lines-derived hepatocytes (HPS0045, HPS0049, HPS0053, and HPS2807).** Data are shown as mean  $\pm$  SEM (n=4). P-values were determined by two-tailed Student's *t*-test for paired samples from each cell line.

While we did not find the similar effect of ATRA on the oleic acid-treated WTC11-derived hepatocytes as that of WD-Hep (**Fig. 27A-D**). We did not find the significant difference for the lipid accumulation between the ATRA treated group

and the control group for both of the WD-specific hepatocyte group and WTC11 iPSC derived hepatocyte group (data was not shown).

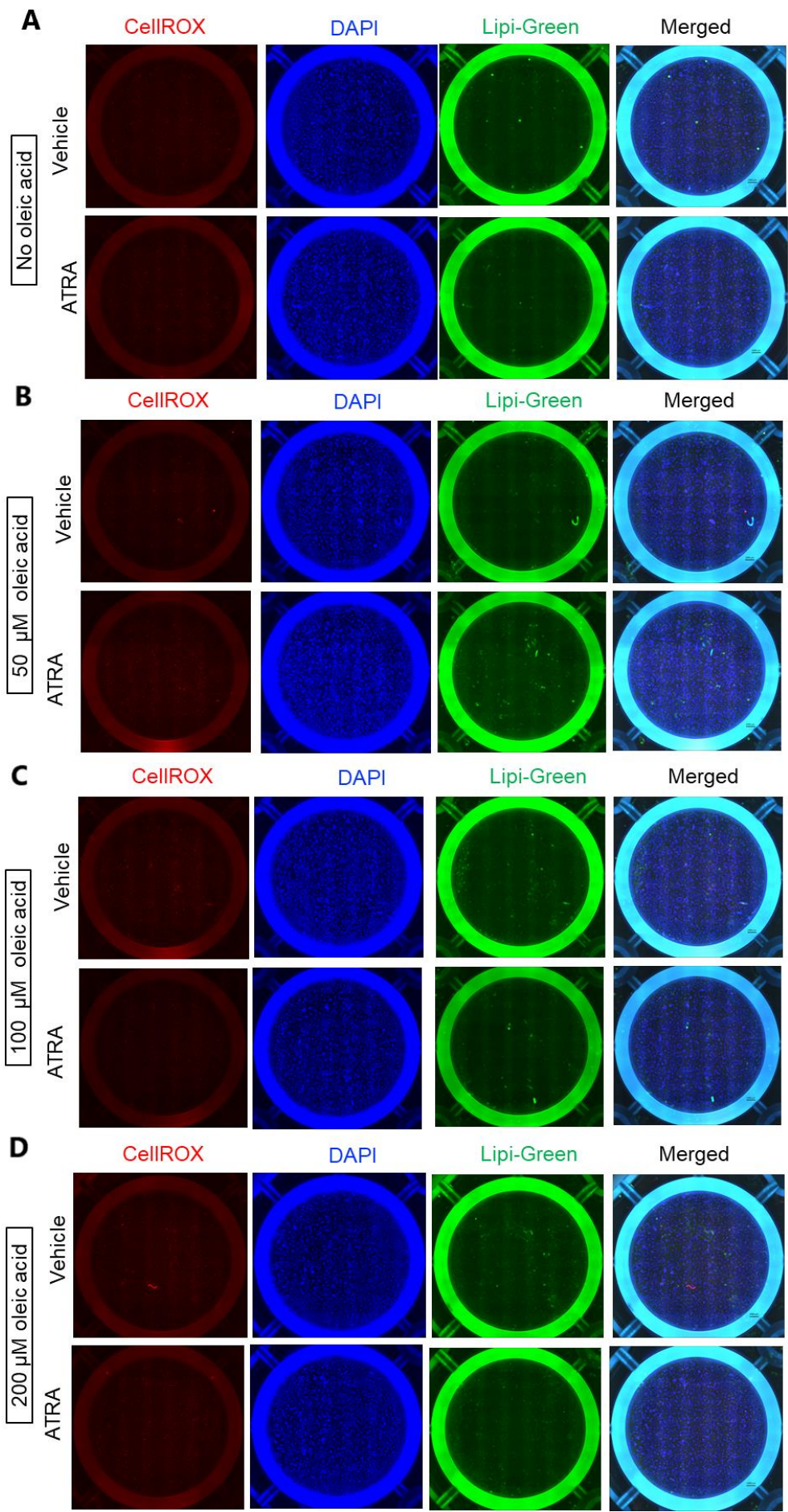


**Figure 27. Tiled whole-well fluorescent images to evaluate ROS production and lipid accumulation in WTC11 iPSC derived hepatocyte. A-D.** Tiled whole-well fluorescent images of CellROX, DAPI and Lipi-Green in WTC11-derived hepatocytes on differentiation day 19 after oleic acid treatment at different concentrations for 8 days with or without ATRA for 4 days. Scale bar is 1000  $\mu\text{m}$ .

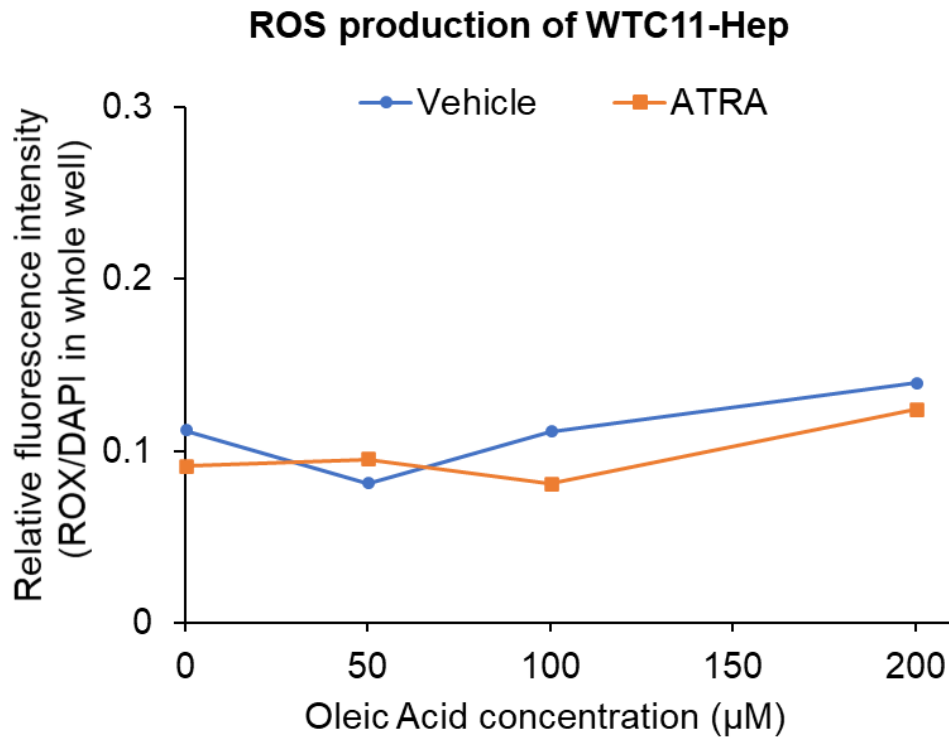


**Figure 28. Quantified ROS production in WTC11-derived hepatocytes.**

Additionally, I further examined the effect of oleic acid on hepatic markers expression with RT-qPCR. The results should that expression of hepatic marker genes, such as ALB, AFP, A1AT and CP, was downregulated by the high concentration (200  $\mu$ M) of oleic acid treatment in WD-specific hepatocytes (**Fig. 29A**), but not in WTC11-derived hepatocytes (**Fig. 29B**). These results indicated that hepatic function of WD-specific hepatocyte was more susceptible to the high oleic acid treatment than that of the WTC iPSC derived hepatocyte.

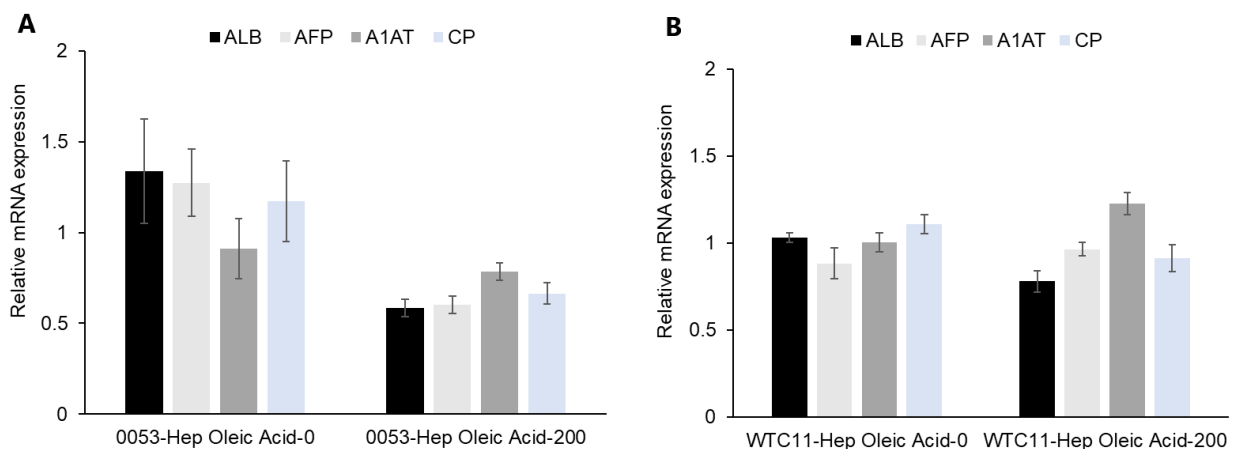


**Figure 29. Hepatic gene expression in WD-iPSC-derived hepatocyte after oleic acid treatment.** Gene expression of *ALB*, *AFP*, *A1AT* and *CP* in HPS0053-derived hepatocytes (**A**) and WTC11-derived hepatocytes (**B**) on differentiation day 17 after treated with or without oleic acid (200  $\mu$ M) for 6 days were analyzed by RT-qPCR (n=3). Bar graphs show the mean  $\pm$  SEM.

## 5. Discussion

In this study, I found that ATRA and some other clinically-approved retinoids could rescue the decreased expression and secretion of Cp in WD-specific hepatocytes. Because the low Cp secretion level is critical for WD diagnose and also a potential contributor for the neurological disease feature of WD, this finding suggested that retinoids could be the promising therapeutic drugs to prevent aggravation of WD.

Furthermore, with the steatosis modeling of WD-Hep, I found that ATRA could alleviate ROS production in WD-specific hepatocytes when exposure to high concentration of oleic acid. It implied the therapeutic value of RA in the fatty liver disease which has been shown by a large part of WD patients. This therapeutic value of RA was also supported by previous studies using genetically modified animals. The loss of RA signaling in mouse liver resulted in steatohepatitis and liver tumors, and feeding on a high RA diet rescued hepatic abnormalities and prevented liver tumors [50]. RA also exhibited suppressive effects on iron-induced oxidative stress in the same transgenic mouse [51]. Also, ATRA effectively improves liver steatosis in a rabbit model of high fat [52]. In *Atp7b* (-/-) mice, the activity of LXR (liver X receptor)/RXR pathway decreases [20], and the activation of these pathways or the feeding of zinc-enriched diet could ameliorate liver damages [18, 19, 53]. Together with our transcriptome analysis data on WD-specific hepatocytes, which showed decreased RA signaling pathway and

increased lipid metabolism, the findings in my present study provide the new evidences of the efficacy of retinoids in preventing hepatic steatosis by using patient-derived hepatocyte models.

Four compound heterozygous mutations carrying WD patient iPSC lines, one ATP7B-KO iPSC line, and one R778L homozygous mutation carrying iPSC line with its genetic heterozygously corrected line [24] were used in this study. Some of the mutations were not previously reported, nor the complicated compound effects of these combinations of the mutations. Thus, their genotype-phenotype correlations were still unclear. Previous studies using WD-specific iPSCs, which used only one patient line each, majorly focused on the expression, localization, and functionality of ATP7B and the cellular toxicity. This approach can be useful to explain the etiology for the single hot spot mutation, while it is unapplicable to study the compound mutation carrying WD iPSC lines. Instead, my study demonstrated that the common pathological mechanisms of WD can be obtained from the integrative approaches using various genotypes in *ATP7B* gene. It provided a convenient platform to explore the therapeutic drugs for the disease treatment.

My results showed Cp expression and secretion are robustly decreased in WD-specific hepatocytes. Since low Cp concentration in the plasma is also a general clinical feature of WD, this finding represented a successful recapitulation of WD phenotype with patient iPSC derived hepatocyte *in vitro*. Interestingly, not only Cp secretion level but also mRNA expression level of Cp was down-regulated in

WD-specific hepatocytes. These results cannot be explained by the common concept that apo-ceruloplasmin has weak protein stability compared to holo-ceruloplasmin, in which copper ion is delivered by ATP7B. Indeed, a previous study reported that Cp mRNA expression in the liver sample of WD patients was decreased [54]. Decreased Cp mRNA must be regulated by other mechanisms in WD-specific hepatocytes. Also, Cp expression was reported to be decreased by an mRNA decay mechanism in response to the intracellular oxidative stress [55]. Thus, decreased Cp mRNA expression in WD-specific hepatocytes might be caused by the abnormal oxidative stress and/or nuclear receptor signaling pathways. It still needs further investigation to illustrate the related regulatory mechanism involved this process.

The drug screening strategy in this study is based on that Cp was proven as a faithful WD disease feature not only in clinic, but also being recapitulated by WD-specific hepatocytes. Cp is a serum ferroxidase, and copper ions incorporation is necessary for its activity during iron metabolism. The critical role of Cp in iron metabolism of neurological system could be helpful to explain that almost half WD patients showing neurodegenerative symptoms. Thus, we assumed that ATRA might be especially helpful to prevent neurological symptom occurrence in WD patients.

Interestingly, my study also provided a potential therapeutic approach for aceruloplasminemia treatment. Aceruloplasminemia is a monogenic disease,

caused by the defective *CP* gene. Patients who suffered from this disease are also showing low Cp secretion. Aceruloplasminemia patients usually presented neurological symptoms, which were considered being resulted from the defective Cp lack of the activity in the iron homeostasis. The critical role of the Cp in neurological system has been investigated[56, 57]. Ceruloplasmin replacement therapy could alleviate the neurological symptoms in aceruloplasminemia[58]. Thus, we assumed that ATRA could be helpful to release the aceruloplasminemia related symptoms via up-regulating Cp expression.

To avoid the variation of the differentiation capability among different iPSC lines, RNA-sequencing was performed to investigate the global gene expression changes of the patient iPSC-derived hepatocyte. Enrichment analyses were further carried out based on the dysregulated gene set in the WD-Hep. Enrichment results suggested that the fatty liver disease-related pathways were dysregulated in WD-Hep. These results implied the possible correlation between copper metabolic disorder and lipid metabolic disorder. While it still needs further investigation for the related mechanisms.

Cp secretion-based drug screening assay and a ROS detection assay platform were developed using human iPSC-derived hepatocytes in my study. The strategy may represent a faithful recapitulation of initial cellular features of WD-specific hepatocytes and thus provide effective platforms to develop potential therapeutics for hepatic steatosis in WD and other fatty liver diseases as well as

to examine the molecular pathogenesis of WD. Because the detection methods are clear and easy, these assays should be further sophisticated to allow high throughput screening systems to identify the ideal therapeutic drugs in the future.

## 6. Reference paper

- [1] A. Ala, A.P. Walker, K. Ashkan, J.S. Dooley, M.L. Schilsky, Wilson's disease, *Lancet* 369(9559) (2007) 397-408.
- [2] C. Arioz, Y. Li, P. Wittung-Stafshede, The six metal binding domains in human copper transporter, ATP7B: molecular biophysics and disease-causing mutations, *Biometals* 30(6) (2017) 823-840.
- [3] D. Huster, A. Kuhne, A. Bhattacharjee, L. Raines, V. Jantsch, J. Noe, W. Schirrmeister, I. Sommerer, O. Sabri, F. Berr, J. Mossner, B. Stieger, K. Caca, S. Lutsenko, Diverse functional properties of Wilson disease ATP7B variants, *Gastroenterology* 142(4) (2012) 947-956 e5.
- [4] A. Gomes, G.V. Dedoussis, Geographic distribution of ATP7B mutations in Wilson disease, *Ann Hum Biol* 43(1) (2016) 1-8.
- [5] O. Bandmann, K.H. Weiss, S.G. Kaler, Wilson's disease and other neurological copper disorders, *Lancet Neurol* 14(1) (2015) 103-113.
- [6] G.J. Brewer, Zinc and tetrathiomolybdate for the treatment of Wilson's disease and the potential efficacy of anticopper therapy in a wide variety of diseases, *Metallomics* 1(3) (2009) 199-206.
- [7] D. Huster, T.D. Purnat, J.L. Burkhead, M. Ralle, O. Fiehn, F. Stuckert, N.E. Olson, D. Teupser, S. Lutsenko, High copper selectively alters lipid metabolism and cell cycle machinery in the mouse model of Wilson disease, *J Biol Chem* 282(11) (2007) 8343-55.
- [8] Y. Kusuda, K. Hamaguchi, T. Mori, R. Shin, M. Seike, T. Sakata, Novel mutations of the ATP7B gene in Japanese patients with Wilson disease, *J Hum Genet* 45(2) (2000) 86-91.
- [9] L. European Association for Study of, EASL Clinical Practice Guidelines: Wilson's disease, *J Hepatol* 56(3) (2012) 671-85.
- [10] G.J. Brewer, Zinc acetate for the treatment of Wilson's disease, *Expert Opin Pharmacother* 2(9) (2001) 1473-7.

- [11] E.A. Roberts, M.L. Schilsky, D. American Association for Study of Liver, Diagnosis and treatment of Wilson disease: an update, *Hepatology* 47(6) (2008) 2089-111.
- [12] P. Ferenci, K. Caca, G. Loudianos, G. Mieli-Vergani, S. Tanner, I. Sternlieb, M. Schilsky, D. Cox, F. Berr, Diagnosis and phenotypic classification of Wilson disease, *Liver Int* 23(3) (2003) 139-42.
- [13] E.V. Polishchuk, M. Concilli, S. Iacobacci, G. Chesi, N. Pastore, P. Piccolo, S. Paladino, D. Baldantoni, I.S.C. van, J. Chan, C.J. Chang, A. Amoresano, F. Pane, P. Pucci, A. Tarallo, G. Parenti, N. Brunetti-Pierri, C. Settembre, A. Ballabio, R.S. Polishchuk, Wilson disease protein ATP7B utilizes lysosomal exocytosis to maintain copper homeostasis, *Dev Cell* 29(6) (2014) 686-700.
- [14] P.V. van den Berghe, J.M. Stapelbroek, E. Krieger, P. de Bie, S.F. van de Graaf, R.E. de Groot, E. van Beurden, E. Spijker, R.H. Houwen, R. Berger, L.W. Klomp, Reduced expression of ATP7B affected by Wilson disease-causing mutations is rescued by pharmacological folding chaperones 4-phenylbutyrate and curcumin, *Hepatology* 50(6) (2009) 1783-95.
- [15] H. Rauch, Toxic Milk, a New Mutation Affecting Copper-Metabolism in the Mouse, *J Hered* 74(3) (1983) 141-144.
- [16] M.C. Yoshida, R. Masuda, M. Sasaki, N. Takeichi, H. Kobayashi, K. Dempo, M. Mori, New mutation causing hereditary hepatitis in the laboratory rat, *J Hered* 78(6) (1987) 361-5.
- [17] K. Terada, T. Sugiyama, The Long-Evans Cinnamon rat: an animal model for Wilson's disease, *Pediatr Int* 41(4) (1999) 414-8.
- [18] O.I. Buiakova, J. Xu, S. Lutsenko, S. Zeitlin, K. Das, S. Das, B.M. Ross, C. Mekios, I.H. Scheinberg, T.C. Gilliam, Null mutation of the murine ATP7B (Wilson disease) gene results in intracellular copper accumulation and late-onset hepatic nodular transformation, *Human Molecular Genetics* 8(9) (1999) 1665-1671.
- [19] J.P. Hamilton, L. Koganti, A. Muchenditsi, V.S. Pendyala, D. Huso, J. Hankin, R.C. Murphy, D. Huster, U. Merle, C. Mangels, N. Yang, J.J. Potter, E. Mezey, S. Lutsenko, Activation of liver X receptor/retinoid X receptor pathway ameliorates

- liver disease in *Atp7B*(*-/-*) (Wilson disease) mice, *Hepatology* 63(6) (2016) 1828-41.
- [20] C.R. Wooton-Kee, M. Robertson, Y. Zhou, B.N. Dong, Z. Sun, K.H. Kim, H.L. Liu, Y. Xu, N. Putluri, P. Saha, C. Coarfa, D.D. Moore, A.M. Nuotio-Antar, Metabolic dysregulation in the *Atp7b*(*-/-*) Wilson's disease mouse model, *P Natl Acad Sci USA* 117(4) (2020) 2076-2083.
- [21] J. Zhang, L. Wei, D. Chen, L. Feng, C. Wu, R. Wang, X. Li, Generation of an integration-free induced pluripotent stem cell (iPSC) line (ZZUNEUi003-A) from a Wilson's disease patient harboring a homozygous R778L mutation in *ATP7B* gene, *Stem Cell Res* 41 (2019) 101664.
- [22] J. Zhang, L. Wei, D. Chen, L. Feng, C. Wu, R. Wang, X. Li, H. Liu, Generation of an integration-free induced pluripotent stem cell (iPSC) line (ZZUNEUi004-A) from a Wilson's disease patient harboring a homozygous Pro992Leu mutation in *ATP7B* gene, *Stem Cell Res* 44 (2020) 101741.
- [23] L. Wei, J. Zhang, D. Chen, L. Feng, C. Wu, R. Wang, X. Li, Generation of an integration-free induced pluripotent stem cell (iPSC) line (ZZUNEUi005-A) from a Wilson's disease patient harboring a homozygous Pro992Leu mutation in *ATP7B* gene, *Stem Cell Res* 47 (2020) 101909.
- [24] S.Q. Zhang, S. Chen, W. Li, X.P. Guo, P. Zhao, J.Y. Xu, Y. Chen, Q. Pan, X.R. Liu, D. Zychlinski, H. Lu, M.D. Tortorella, A. Schambach, Y. Wang, D.Q. Pei, M.A. Esteban, Rescue of *ATP7B* function in hepatocyte-like cells from Wilson's disease induced pluripotent stem cells using gene therapy or the chaperone drug curcumin, *Human Molecular Genetics* 20(16) (2011) 3176-3187.
- [25] F. Yi, J. Qu, M. Li, K. Suzuki, N.Y. Kim, G.H. Liu, J.C.I. Belmonte, Establishment of hepatic and neural differentiation platforms of Wilson's disease specific induced pluripotent stem cells, *Protein Cell* 3(11) (2012) 855-863.
- [26] S. Parisi, E.V. Polishchuk, S. Allocca, M. Ciano, A. Musto, M. Gallo, L. Perone, G. Ranucci, R. Iorio, R.S. Polishchuk, S. Bonatti, Characterization of the most frequent *ATP7B* mutation causing Wilson disease in hepatocytes from patient induced pluripotent stem cells, *Sci Rep-Uk* 8 (2018).

- [27] A.W. Overeem, K. Klappe, S. Parisi, P. Kloters-Planchy, L. Matakovic, M.D. Espina, C.A. Drouin, K.H. Weiss, S.C.D. van Ijzendoorn, Pluripotent stem cell-derived bile canaliculi-forming hepatocytes to study genetic liver diseases involving hepatocyte polarity, *Journal of Hepatology* 71(2) (2019) 344-356.
- [28] J. Petters, C. Cimmaruta, K. Iwanov, M.L. Chang, C. Volkner, G. Knuebel, H.M. Escobar, M.J. Frech, A. Hermann, A. Rolfs, J. Lukas, Generation of induced pluripotent stem cell lines AKOSi002-A and AKOSi003-A from symptomatic female adults with Wilson disease, *Stem Cell Research* 43 (2020).
- [29] A.J. Coffey, M. Durkie, S. Hague, K. McLay, J. Emmerson, C. Lo, S. Klaffke, C.J. Joyce, A. Dhawan, N. Hadzic, G. Mieli-Vergani, R. Kirk, K. Elizabeth Allen, D. Nicholl, S. Wong, W. Griffiths, S. Smithson, N. Giffin, A. Taha, S. Connolly, G.T. Gillett, S. Tanner, J. Bonham, B. Sharrack, A. Palotie, M. Rattray, A. Dalton, O. Bandmann, A genetic study of Wilson's disease in the United Kingdom, *Brain* 136(Pt 5) (2013) 1476-87.
- [30] M. Sato, J.D. Gitlin, Mechanisms of copper incorporation during the biosynthesis of human ceruloplasmin, *J Biol Chem* 266(8) (1991) 5128-34.
- [31] N.E. Hellman, J.D. Gitlin, Ceruloplasmin metabolism and function, *Annu Rev Nutr* 22 (2002) 439-58.
- [32] A. Saha, A. Karnik, N. Sathawara, P. Kulkarni, V. Singh, Ceruloplasmin as a marker of occupational copper exposure, *J Expo Sci Env Epid* 18(3) (2008) 332-337.
- [33] A.L.P. Chapman, T.J. Mocatta, S. Shiva, A. Seidel, B. Chen, I. Khalilova, M.E. Paumann-Page, G.N.L. Jameson, C.C. Winterbourn, A.J. Kettle, Ceruloplasmin Is an Endogenous Inhibitor of Myeloperoxidase, *Journal of Biological Chemistry* 288(9) (2013) 6465-6477.
- [34] K. Okita, T. Yamakawa, Y. Matsumura, Y. Sato, N. Amano, A. Watanabe, N. Goshima, S. Yamanaka, An Efficient Nonviral Method to Generate Integration-Free Human-Induced Pluripotent Stem Cells from Cord Blood and Peripheral Blood Cells, *Stem Cells* 31(3) (2013) 458-466.
- [35] K. Okita, Y. Matsumura, Y. Sato, A. Okada, A. Morizane, S. Okamoto, H. Hong, M. Nakagawa, K. Tanabe, K. Tezuka, T. Shibata, T. Kunisada, M.

- Takahashi, J. Takahashi, H. Saji, S. Yamanaka, A more efficient method to generate integration-free human iPS cells, *Nat Methods* 8(5) (2011) 409-U52.
- [36] M. Nakagawa, Y. Taniguchi, S. Senda, N. Takizawa, T. Ichisaka, K. Asano, A. Morizane, D. Doi, J. Takahashi, M. Nishizawa, Y. Yoshida, T. Toyoda, K. Osafune, K. Sekiguchi, S. Yamanaka, A novel efficient feeder-free culture system for the derivation of human induced pluripotent stem cells, *Sci Rep-Uk* 4 (2014).
- [37] M. Frydman, B. Bonnetamir, L.A. Farrer, P.M. Conneally, A. Magazanik, S. Ashbel, Z. Goldwicht, Assignment of the Gene for Wilson Disease to Chromosome-13 - Linkage to the Esterase-D Locus, *P Natl Acad Sci USA* 82(6) (1985) 1819-1821.
- [38] R.E. Tanzi, K. Petrukhin, I. Chernov, J.L. Pellequer, W. Wasco, B. Ross, D.M. Romano, E. Parano, L. Pavone, L.M. Brzustowicz, M. Devoto, J. Peppercorn, A.I. Bush, I. Sternlieb, M. Pirastu, J.F. Gusella, O. Evgrafov, G.K. Penchaszadeh, B. Honig, I.S. Edelman, M.B. Soares, I.H. Scheinberg, T.C. Gilliam, The Wilson Disease Gene Is a Copper Transporting Atpase with Homology to the Menkes Disease Gene, *Nat Genet* 5(4) (1993) 344-350.
- [39] R. Siller, S. Greenhough, E. Naumovska, G.J. Sullivan, Small-Molecule-Driven Hepatocyte Differentiation of Human Pluripotent Stem Cells, *Stem Cell Reports* 4(5) (2015) 939-952.
- [40] F.A. Ran, P.D. Hsu, J. Wright, V. Agarwala, D.A. Scott, F. Zhang, Genome engineering using the CRISPR-Cas9 system, *Nat Protoc* 8(11) (2013) 2281-2308.
- [41] G. Duester, A. Molotkov, F.A. Mic, Retinoid activation of retinoic acid receptors but not retinoid X receptors is sufficient for mouse embryonic development, *Faseb J* 17(5) (2003) A779-A780.
- [42] D.J. Mangelsdorf, E.S. Ong, J.A. Dyck, R.M. Evans, Nuclear Receptor That Identifies a Novel Retinoic Acid Response Pathway, *Nature* 345(6272) (1990) 224-229.
- [43] S. Nkongolo, L. Nussbaum, F.A. Lempp, H. Wodrich, S. Urban, Y. Ni, The retinoic acid receptor (RAR) alpha-specific agonist Am80 (tamibarotene) and other RAR agonists potently inhibit hepatitis B virus transcription from cccDNA, *Antiviral Res* 168 (2019) 146-155.

- [44] R.A. Chandraratna, Tazarotene--first of a new generation of receptor-selective retinoids, *Br J Dermatol* 135 Suppl 49 (1996) 18-25.
- [45] A. Mounier, D. Georgiev, K.N. Nam, N.F. Fitz, E.L. Castranio, C.M. Wolfe, A.A. Cronican, J. Schug, I. Lefterov, R. Koldamova, Bexarotene-Activated Retinoid X Receptors Regulate Neuronal Differentiation and Dendritic Complexity, *J Neurosci* 35(34) (2015) 11862-76.
- [46] F. Zapata-Gonzalez, F. Rueda, J. Petriz, P. Domingo, F. Villarroya, J. Diaz-Delfin, M.A. de Madariaga, J.C. Domingo, Human dendritic cell activities are modulated by the omega-3 fatty acid, docosahexaenoic acid, mainly through PPAR(gamma):RXR heterodimers: comparison with other polyunsaturated fatty acids, *J Leukoc Biol* 84(4) (2008) 1172-82.
- [47] T. Wilkins, A. Tadmok, I. Hepburn, R.R. Schade, Nonalcoholic Fatty Liver Disease: Diagnosis and Management, *Am Fam Physician* 88(1) (2013) 35-42.
- [48] J. Seessle, A. Gohdes, D.N. Gotthardt, J. Pfeiffenberger, N. Eckert, W. Stremmel, U. Reuner, K.H. Weiss, Alterations of lipid metabolism in Wilson disease, *Lipids Health Dis* 10 (2011) 83.
- [49] Z. Chen, R. Tian, Z. She, J. Cai, H. Li, Role of oxidative stress in the pathogenesis of nonalcoholic fatty liver disease, *Free Radic Biol Med* 152 (2020) 116-141.
- [50] A. Yanagitani, S. Yamada, S. Yasui, T. Shimomura, R. Murai, Y. Murawaki, K. Hashiguchi, T. Kanbe, T. Saeki, M. Ichiba, Y. Tanabe, Y. Yoshida, S. Morino, A. Kurimasa, N. Usuda, H. Yamazaki, T. Kunisada, H. Ito, Y. Murawaki, G. Shiota, Retinoic acid receptor alpha dominant negative form causes steatohepatitis and liver tumors in transgenic mice, *Hepatology* 40(2) (2004) 366-75.
- [51] H. Tsuchiya, Y. Akechi, R. Ikeda, R. Nishio, T. Sakabe, K. Terabayashi, Y. Matsumi, A.A. Ashla, Y. Hoshikawa, A. Kurimasa, T. Suzuki, N. Ishibashi, S. Yanagida, G. Shiota, Suppressive effects of retinoids on iron-induced oxidative stress in the liver, *Gastroenterology* 136(1) (2009) 341-350 e8.

- [52] L. Zarei, N. Farhad, A. Abbasi, All-Trans Retinoic Acid (atRA) effectively improves liver steatosis in a rabbit model of high fat induced liver steatosis, *Arch Physiol Biochem* (2020).
- [53] C.R. Wooton-Kee, A.K. Jain, M. Wagner, M.A. Grusak, M.J. Finegold, S. Lutsenko, D.D. Moore, Elevated copper impairs hepatic nuclear receptor function in Wilson's disease, *J Clin Invest* 125(9) (2015) 3449-60.
- [54] M.J. Czaja, F.R. Weiner, S.J. Schwarzenberg, I. Sternlieb, I.H. Scheinberg, D.H. Vanthiel, N.F. Larusso, M.A. Giambrone, R. Kirschner, M.L. Koschinsky, R.T.A. Macgillivray, M.A. Zern, Molecular Studies of Ceruloplasmin Deficiency in Wilsons-Disease, *Journal of Clinical Investigation* 80(4) (1987) 1200-1204.
- [55] N. Tapryal, C. Mukhopadhyay, D. Das, P.L. Fox, C.K. Mukhopadhyay, Reactive Oxygen Species Regulate Ceruloplasmin by a Novel mRNA Decay Mechanism Involving Its 3'-Untranslated Region IMPLICATIONS IN NEURODEGENERATIVE DISEASES, *Journal of Biological Chemistry* 284(3) (2009) 1873-1883.
- [56] B. Wang, X.P. Wang, Does Ceruloplasmin Defend Against Neurodegenerative Diseases?, *Curr Neuropharmacol* 17(6) (2019) 539-549.
- [57] S.J. Texel, X. Xu, Z.L. Harris, Ceruloplasmin in neurodegenerative diseases, *Biochem Soc Trans* 36(Pt 6) (2008) 1277-81.
- [58] A. Zanardi, A. Conti, M. Cremonesi, P. D'Adamo, E. Gilberti, P. Apostoli, C.V. Cannistraci, A. Piperno, S. David, M. Alessio, Ceruloplasmin replacement therapy ameliorates neurological symptoms in a preclinical model of aceruloplasminemia, *Embo Mol Med* 10(1) (2018) 91-106.

## 7. Acknowledgements

I would like to thank Prof. Tatsuya Oda of Gastroenterological and Hepatobiliary Surgery at the University of Tsukuba for his kindly supervise and guidance. He is an open-minded supervisor. As an international student, I especially appreciated his generous support and encouragement when I feel helpless during my study.

I would like to express my appreciation to Dr. Yohei Hayashi, the team leader of the RIKEN BRC iPSC Cell Advanced Characterization and Development Team. Since I joined his lab in the year 2018, I started my study of iPSC. I learned a lot of iPSC skills and scientific paper writing skills from him during the last four years. He is an insightful PI. With his guidance and recommendation, I have the chance to read some valuable books, which are not only helpful for my experimental skills and scientific paper writing improvement but also for my career in the future. I also appreciated his kindly help during my postdoc application. Without his generous support and guidance, I could not complete my Ph.D. program.

I would like to thank Prof. Yunwen Zheng and Prof. Nobuhiro Ohkohchi of Gastroenterological and Hepatobiliary Surgery at the University of Tsukuba for their kindly help during my MEXT scholarship application and supervision.

I would like to express my gratitude to all the team members of the RIKEN BRC iPSC Cell Advanced Characterization and Development Team for their

encouragement and support during my four years of study. I especially would like to thank Kumiko Omori-san. She helped me a lot for my life in RIKEN in the last four years.

I would like to express my gratitude to all the members of Gastroenterological and Hepatobiliary Surgery at the University of Tsukuba for their generous help and support during my four years of study. I especially appreciated Dr. Kinji Furuya for his kindly help and discussion on my presentation slide.